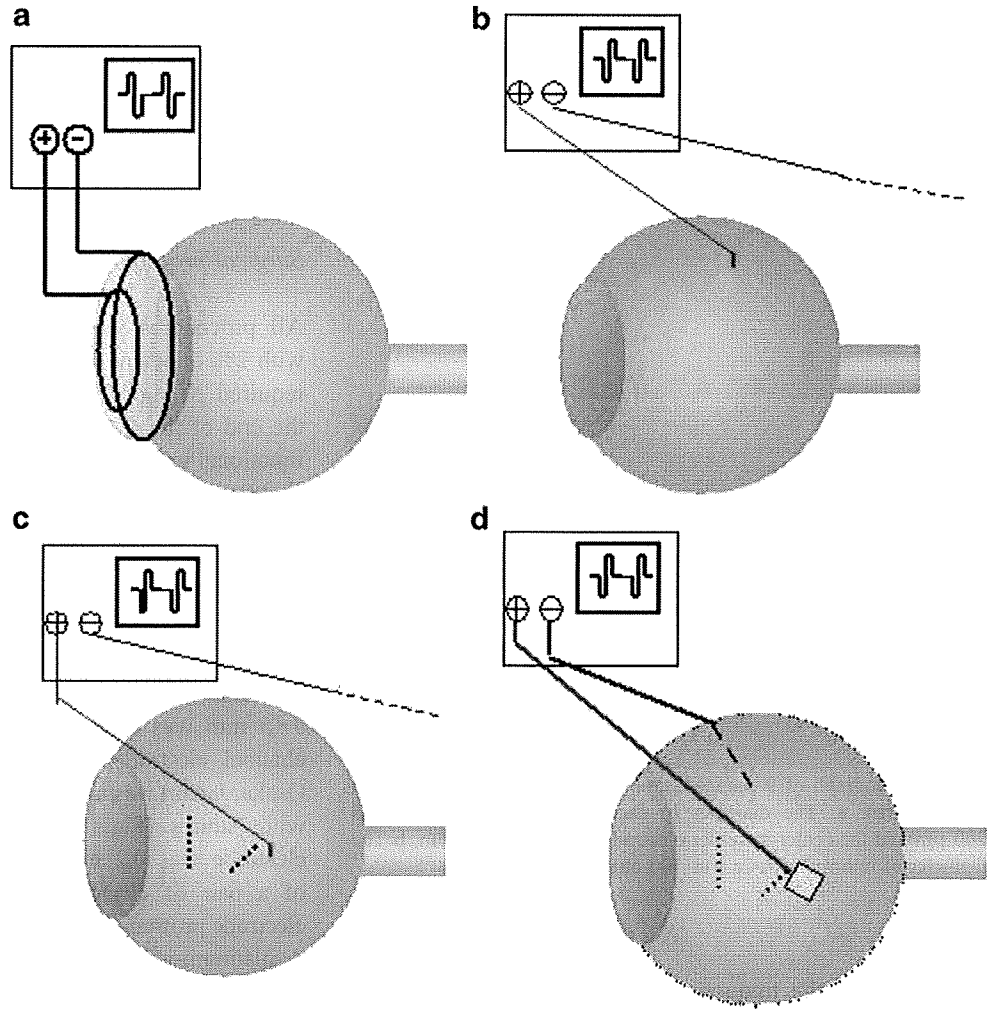

Fig. 1 Schema of different methods to stimulate the retina. **a** Trans-corneal electrical stimulation (TcES); **b** trans-scleral electrical stimulation (TsES); **c** trans-scleral monopolar stimulation in patients; **d** suprachoroidal-transretinal stimulation (STS) in patients

infrared charge-coupled device (CCD) camera and a red light-emitting diode (LED; 660 nm; maximum light power of 10±3 μW; stimulus duration of 0.1 s).

Before inserting the contact lens electrode, the indirect pupillary light reflex was recorded. After inserting the contact lens electrode, the electrically evoked pupillary responses (EEPRs) were recorded from the contralateral eye. The relative amplitude of the EEPR was determined as follows:

$$\text{Relative pupillary constriction(RPC\%)} = 100(a - b)/a$$

where a = pre-stimulus baseline pupil diameter (mm), and b = maximally constricted pupil diameter (mm).

Transscleral electrical stimulation

A stimulating electrode (platinum wire, diameter: 1.0 mm, exposed 1.0 mm at the tip, Unique Medical, Osaka, Japan) was placed on the conjunctiva in the upper temporal quadrant 16 mm to 18 mm from the corneal limbus (Fig. 1b). The conjunctiva was anesthesized with 0.4% oxyburocaine hydrochloride. A return electrode (Ag-AgCl) was placed on the ipsilateral wrist. Pulse trains with charge-balanced biphasic pulses (cathodic first) were applied through the stimulating electrodes.

We examined the relationship between the brightness of phosphenes and the pulse parameters, viz., pulse duration, interpulse delay, frequency and the number of pulse trains, using suprathreshold currents (1.0 to 1.5 mA) (Fig. 2b). Initially, the threshold current to evoke phosphenes was determined with the other parameters fixed at a pulse duration 1 ms, interpulse delay 1 ms, frequency 20 Hz and number of pulses 20. These fixed parameters were chosen based on the results of a preliminary experiment to explore the effective parameters to elicit phosphenes. The relationship between the brightness of the phosphenes and the pulse duration was examined with the injected charge per pulse constant. The pulse duration varied from 0.5 to 4.0 ms while the frequency at 50 Hz and the number of pulses at 20.

The relationship between brightness of the phosphenes and the interpulse delay was examined with the interpulse delay varying from 0 to 4 ms while the pulse duration was

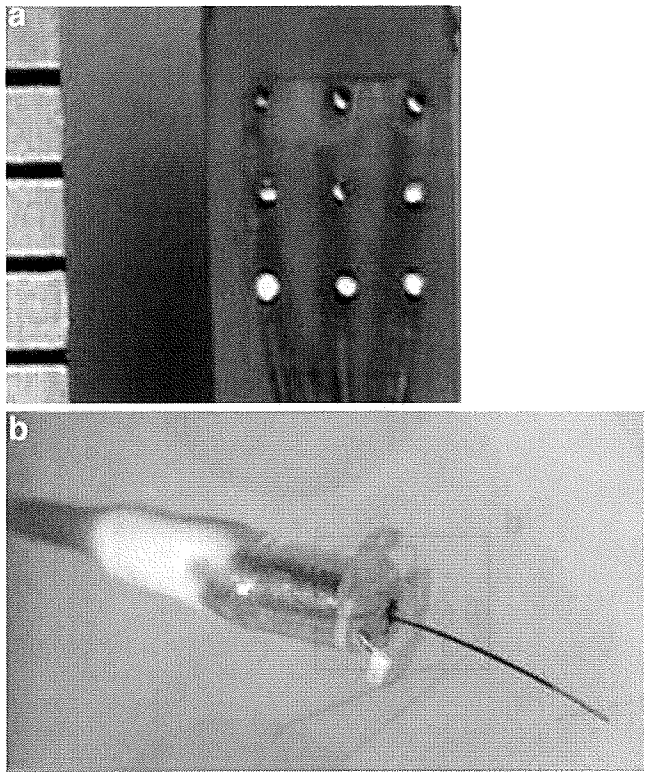

Fig. 2 Photograph of 9-channel stimulating electrode (**a**) and return electrode (**b**). **a**. The diameter of each stimulating electrode was 200 μm and the center-to-center electrode distance was 1 mm. **b** The diameter of return electrode was 100 um

fixed at 1 ms, the frequency at 50 Hz and the number of pulses at 20. The relationship between the brightness of the phosphene and the pulse frequency was examined with the frequency varying from 5 to 100 Hz while the pulse duration was fixed at 1 ms, interpulse delay at 1 ms and the number of pulses at 20. The relationship between brightness of the phosphenes and the number of pulses was also examined with the number of pulses varied from 1 to 50 while the pulse duration was fixed at 1 ms, the interpulse delay at 1 ms and the frequency at 20 Hz.

Subjects were questioned about the brightness and the size of the phosphene for each set of stimulus parameters. The brightness was classified into five grades; the brightest phosphenes during one set of experiments was assigned a value of 5 and the next brightest was 4, and so on. The experiments were conducted systematically with an increase of stimulus parameters (pulse duration, interpulse delay, frequency and the number of pulse trains) with an interval of 5 to 10 s. The number of trials in a unique set of stimulus parameters was generally once, but was two or more when subjects asked for a repetition. Subjects were masked to the test conditions, and the examiner, who was aware of the stimulus conditions, asked questions about the phosphenes. False positive trials (i.e., no stimulus presented) were included to determine the reliability of the responses.

Suprachoroidal-transretinal stimulation in patients with retinitis pigmentosa

Surgical procedure

All procedures were performed under topical anesthesia with 2% lidocaine hydrochloride drops; however, patient 1 required 20 mg of fentanest intravenously at approximately the end of the trial. The total hours including surgery and functional testing was 3 h in patient 1 and 2.5 h in patient 2.

After dissecting the lateral rectus muscle insertion, trial transscleral stimuli were given to determine the scleral area around the insertion of the inferior oblique muscle that consistently evoked low threshold phosphenes (Fig. 1c). The diameter of monopolar platinum electrode was 0.5 mm (Unique Medical, Osaka, Japan). After identifying the low threshold area by monolopar electrode, a scleralpocket of 5×5 mm was created with a crescent knife, and a nine-channel electrode array (size, 4×5 mm, Unique Medical, Osaka, Japan) was inserted into the scleral pocket and secured with sutures (Fig. 1d). The diameter of each platinum electrode was 0.2 mm, and the center-to-center separation of a pair of electrodes was 1 mm. The surface of the electrode protruded from the silicon base by 50 μm (Fig. 2a). A platinum-wire reference electrode (0.1 mm in diameter, 8 mm in length and 3 mm of tip exposed) was inserted into the vitreous cavity through the pars plana (Fig. 2b).

Functional testing

A stimulator was designed to deliver charge-balanced biphasic pulses to individual electrodes simultaneously (Fig. 3a). Biphasic pulses (pulse duration, 0.5 or 1.0 ms; frequency, 20 Hz; interpulse delay, 0.5 ms; number of pulses 20, Fig. 3b) were delivered through the selected channel(s) or combination of multiple channels.

The psychophysical testing was performed under dim room lights. The current stimulation was applied 0.5 s after a conditioning phonic stimulus by a buzzer. The threshold current to perceive a phosphene was determined by increasing the current intensity from 0.1 mA until patients recognized the localized phosphene. The maximum current was limited to 1.0 mA for safety based on the rabbit experiments (Nakauchi et al., ARVO, 2006,47, E-Abstract 3197).

The size and shape of the phosphene that the patients described were recorded. False positive trials (i.e., no stimulus presented) were included to determine the reliability of the responses. The procedure was repeated to

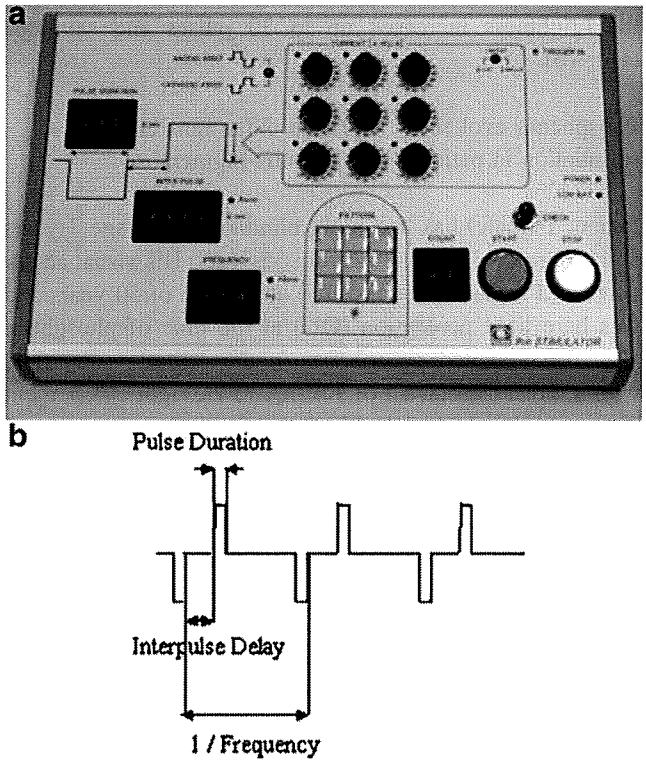

Fig. 3 Photograph of the stimulator for a 9-channel electrode (**a**) and the diagram of stimulating current pulse (**b**). **a** Charge-balanced biphasic pulses were delivered to individual electrodes simultaneously. **b** The first pulse delivers a cathodic current while the second pulse delivers anodic current to balance the charge

identify the threshold current. Care was taken not to influence the description by the patients.

After determining the threshold current of each electrode, simultaneous multi-channel stimulation was performed to examine if patients could achieve two-point discrimination or pattern recognition.

Statistical analyses

Data are presented as the means ± standard error of the means (SEM) and were statistically analyzed with the SPSS 10.0J program (SPSS Inc, Chicago, IL). Comparisons between two groups were made by the Student's *t* test when data were normally distributed or by the Mann-Whitney U test when data were not normally distributed. The degree of correlation was evaluated by the coefficient of correlation (r) calculated using Pearson's correlation coefficient. Comparisons between three groups or more were made by one-way ANOVA followed by the Tukey test when data were normally distributed or by the Dunn's test when data were not normally distributed. The probability level is represented as the value *P*; statistical significance was set at $P<0.05$.

Results

Electrically evoked and light-evoked pupillary responses in normal subjects

Typical pupillary responses from a normal subject are shown in Fig. 4. The waveform of the EEPR was similar to that of the light response, but the amplitude of the EEPR was smaller than that of the light response. The mean latency of the EEPR (at 150 μA; 10 ms duration; 20 Hz; 20 pulses) was 0.29±0.01 s and that of the light response (660 nm; maximum light power of 10±3 μW; stimulus duration of 0.1 s) was 0.33±0.01 s. This difference was significant ($P<0.01$, Student's *t* test).

The relationship between the current intensity and EEPR was examined with stimuli of 20 Hz, 10 ms duration, and 20 pulses while the current intensity was varied from 25 μA to 250 μA. A RPC greater than 3% was obtained at currents ≥150 μA and the mean RPC was 6.3±1.1%. A highly significant positive correlation was found between the current intensity and the RPC amplitude ($r=0.98$ and $P<0.01$; Pearson's correlation coefficient, Fig. 5a).

We then examined the relationship between the frequency of the pulses and the EEPR at 150 μA, 10 ms duration and 20 pulses while the frequency of pulses varied from 5 Hz to 50 Hz. Although the mean RPC amplitude of the EEPR was very small at frequencies lower than 10 Hz, the mean RPC reached a peak of 7.9±1.9% at 20 Hz. Increasing the frequency up to 50 Hz resulted in a decrease in the RPC to 3.9±1.5% at 50 Hz (Fig. 5b).

The subjective phosphenes were brighter at frequencies between 15 and 33 Hz compared with those elicited by frequencies lower than 15 Hz or higher than 33 Hz.

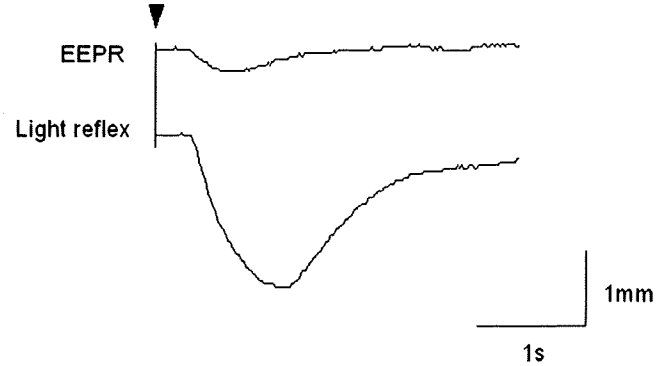

Fig. 4 Electrically evoked (upper) and light-evoked (lower) indirect pupillary responses elicited by electrical stimulation or light stimulation. The amplitude of the EEPR was smaller than that of light reflex, but the shape of the waveform is similar to that of light response

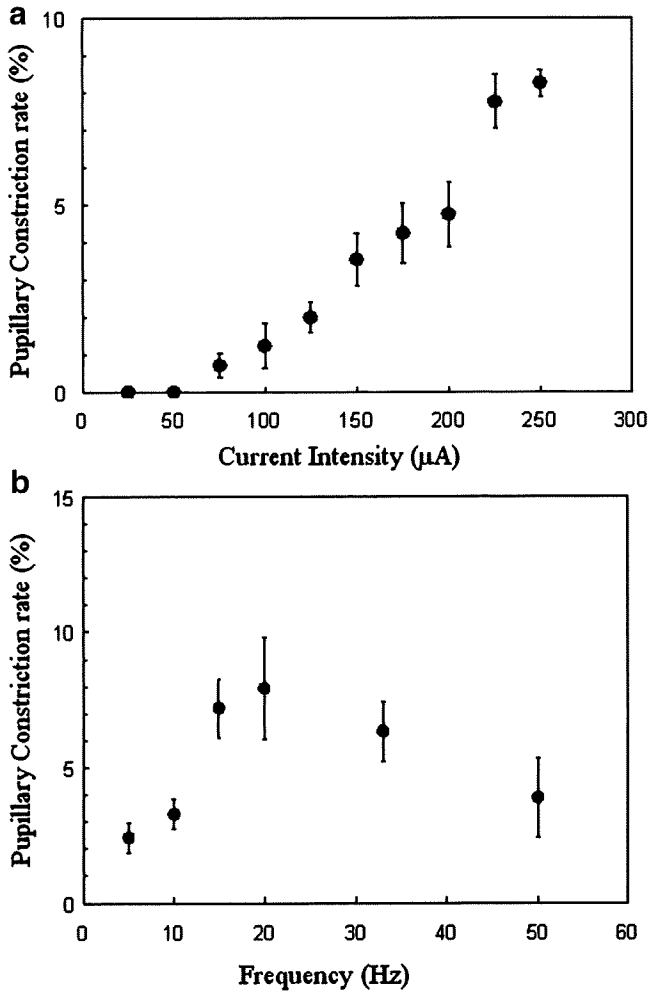

Fig. 5 Characteristics of pupillary constrictions elicited by transcorneal electrical stimulation. **a** Relative pupillary constriction amplitudes are plotted against the current intensity in normal subjects. The average pupillary constriction amplitude increases as the current intensity increases. **b** Relative pupillary constriction amplitudes are plotted against the frequency of electrical stimulation in normal subjects. A bandpass-shaped increase of pupillary constriction amplitude is observed. Bar represents standard error

Phosphenes evoked by trans-scleral electrical stimulation

All subjects reported a localized, round-shaped phosphene in response to TsES. The position of the phoshenes corresponded to the retinal loci where phoshenes were evoked by indenting the scleral electrode. Generally, shorter pulse durations elicited more localized phosphenes. The brightness of the phosphenes decreased with an increase of pulse duration in which the injected charge per pulse was kept constant (Fig. 6a). An increase in the interpulse delay also increased the perceived brightness of the phosphenes and was almost saturated at 1 ms (Fig. 6b). The brightness of the phosphenes increased with an increase in the pulse frequency up to 20 Hz and peaked at 50 Hz, but decreased at 100 Hz (Fig. 7a). With an increase in the pulse number, the brightness increased up to 20 pulses and saturated (Fig. 7b).

Phosphenes evoked by suprachoroidal-transretinal stimulation in patients with retinitis pigmentosa

Patient 1 (male) has had night blindness since age 7 years and progressive visual loss from 35 years. His visual acuity decreased to hand motion (OU) at the age of 50 years and was bare light perception (OU) at the time of phosphene test. TcES elicited phosphenes in the central visual field with a threshold current of 1.4 mA in the right eye. Patient 2 (female) has had night blindness from age 15 years and progressive visual loss from 27 years. Her visual acuity decreased to hand motion (OU) at the age of 55 years and was bare light perception (OD), and was 0 (OS) at the time of phosphene test. TcES elicited phosphenes that were perceived in the central visual field with a threshold current of 1.1 mA in the right eye.

Examination of the ocular fundus of the two patients with RP revealed extensive retinal degeneration including

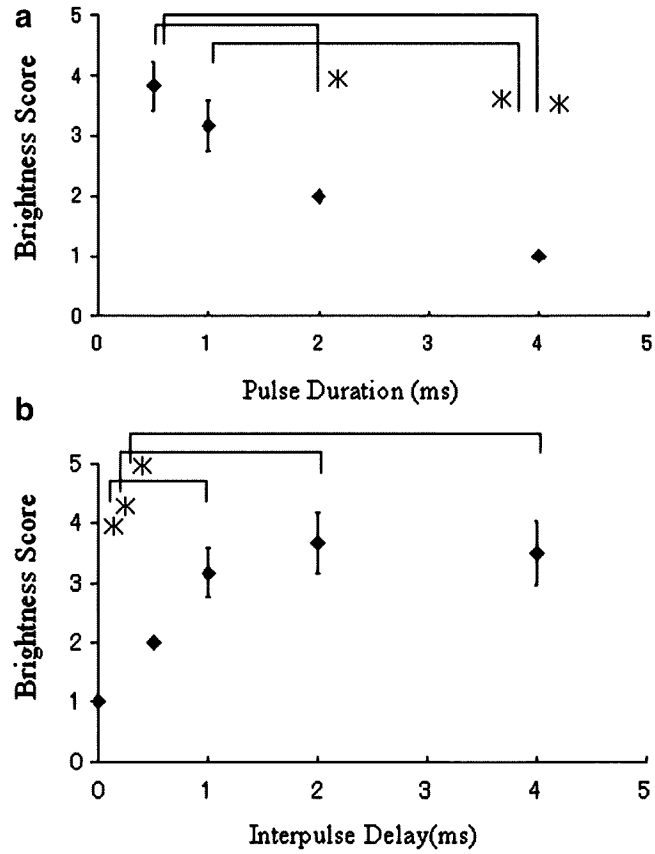

Fig. 6 The relationship between the brightness of phosphenes and pulse duration (**a**) and interpulse delay (**b**). **a** The brightness of phosphenes decreases with an increase of pulse duration (the total injected charge was constant). **b** The application of interpulse delay increased the perceived brightness of phosphene and almost saturated at 1 ms

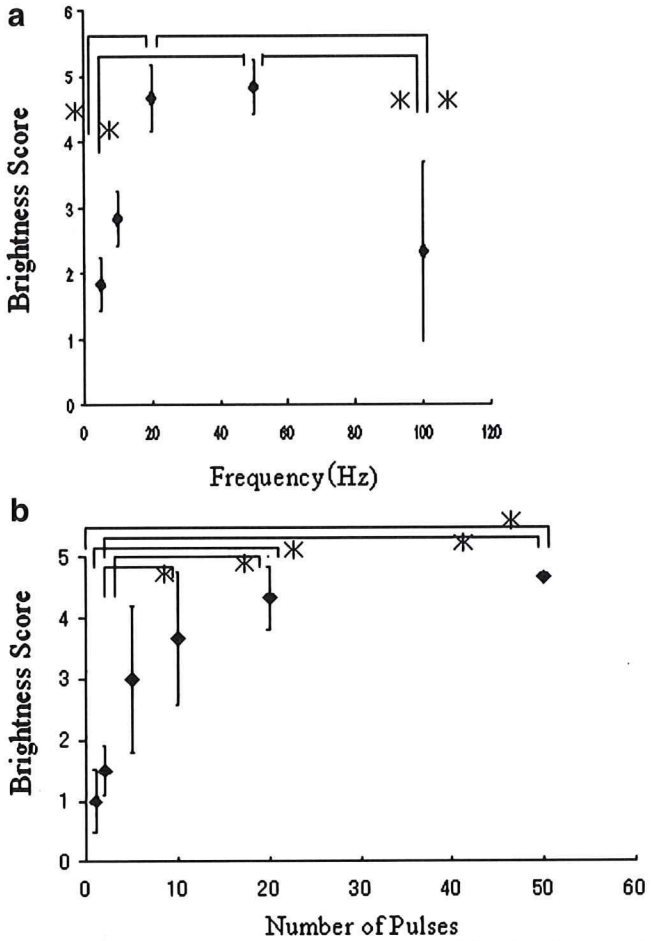

Fig. 7 The relationship between the brightness of the phosphenes and the pulse frequency (**a**) and the number of pulses (**b**). **a** The brightness of the phophenes increased with the increase of pulse frequency up to 20 Hz and peaked at 50 Hz, but decreased at 100 Hz. **b** With the increase of pulse number, the brightness increased up to 20 pulses and saturated. Bar represents standard error. $*P<0.05$

the macular and peripheral retina (Fig. 8). Trans-scleral monopolar stimulation revealed a confined low threshold area (0.4 mA, duration 1 ms) about 2 mm posterior to the inferior muscle insertion in patient 1. In patient 2, phosphenes were evoked from only a confined area about 2 mm posterior to the inferior muscle insertion with the maximum electrical current (1 mA, duration 1 ms).

By stimulating a single channel of nine electrodes with STS, localized phosphenes were obtained with stimuli of 0.3–0.5 mA (duration,0.5 ms: 0.48–0.80 mC/cm2) in patient 1 and 0.4 mA (duration,1.0 ms: 1.27 mC/cm2) in patient 2. Phosphenes were not reported from false-positive trials. Due to the difficulty in obtaining the results, only qualitative data can be provided in psychophysical experiments. The size of phosphene varied from a dime to a quarter coin at a distance of a stretched arm depending on the channel stimulated in both patients. Dumbbell-shaped phosphenes were perceived when the stimuli were delivered through two adjacent channels in both patients. Two dumbbell-shaped phosphenes oriented in different directions were perceived by stimulating different pairs of channels in patient 1.

Discussion

We have determined the efficient parameters to stimulate the retina by extraocular electrical stimuli. For TcES, two concentric ring electrodes were placed on the corneal surface and a current between the two rings has been reported to stimulate the peripheral retina by lower electrical currents and the macular area by higher currents [11]. The EEPR was used to evaluate the frequency dependence of TcES.

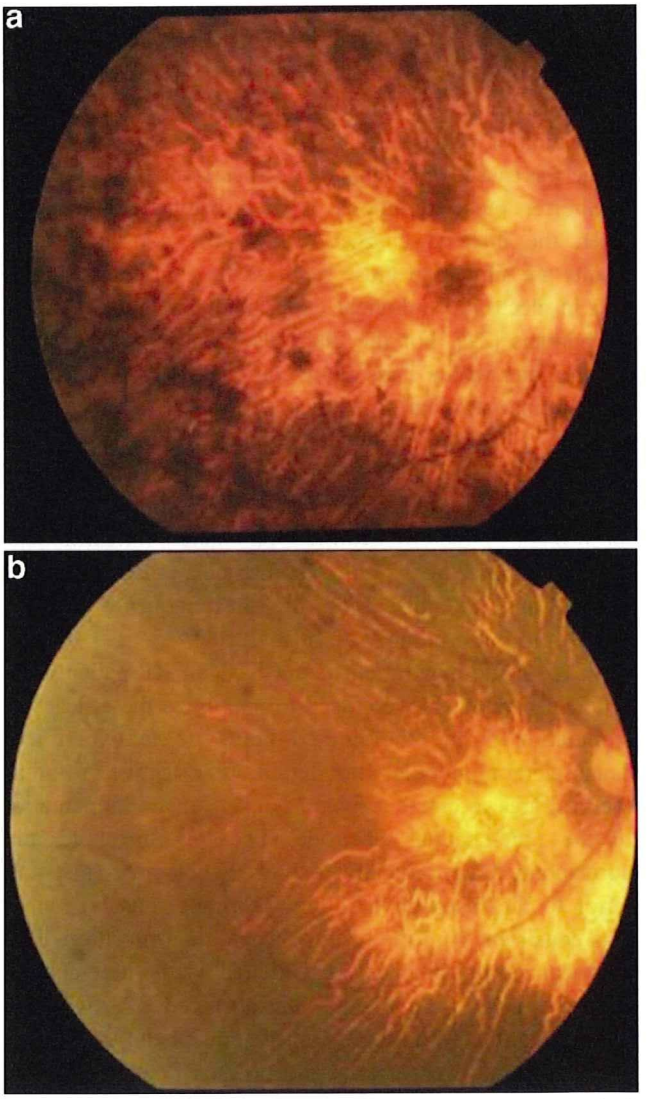

Fig. 8 Fundus photos of patient 1 (**a**) and patient 2 (**b**). In both patients, retinal degeneration can be seen in the macular area as well as in the peripheral retina

The relative amplitude of constriction of the EEPR increased as the current intensity increased, and the amplitude was largest at 20 Hz (Fig. 5). The perceived phosphene also became brighter around this frequency. These results together with previous reports [18, 28] suggest that a frequency around 20 Hz is the most effective frequency to stimulate the retina. The frequency dependency of the intensity of the phosphenes has not been explicitly reported, but for epiretinal stimulation, 20 Hz was used [22].

A possibility that a direct current affected the pupil efferent and elicited the EEPR was eliminated by the report that an EEPR cannot be elicited from the contralateral healthy eye from electrically stimulating an eye with optic atrophy [28].

The efficient parameters for localized extraocular stimulation for TsES were determined in normal subjects. The frequency dependence of the phosphene intensity showed a bandpass-shaped curve (Fig. 7), which was similar to the result of TcES. The peak EEPR was elicited by 20 Hz for TcES, while that for a subjective phophene was 50 Hz for TsES. This discrepancy may be because the EEPR was produced by the stimulation of W type RGCs [26], while the subjective phosphene was caused by X (alpha) or Y (beta) type RGCs [12, 26].

Shorter pulse durations elicited brighter phosphenes when the injected charge density was constant. These results are similar to those reported for epiretinal stimulation in electrophysiological experiment on rabbits [9] and on humans [22]. For the interpulse delay, the phosphene was brighter with a 1-ms delay compared with 0 or 0.5 ms. In epiretinal stimulation studies, 10 us to 2 ms were used [6, 22]. Pulse trains evoked brighter phosphenes than single-pulse stimulation. A pulse train (duration, 1.5 s) was also used in the epiretinal stimulation study [22]. From these findings, the efficient pulse parameters for extraocular stimulation in acute experiments may be a pulse duration of 0.5 to 1 ms, interpulse delay of 1 ms, frequency of 20 to 50 Hz and pulse number of 10 to 20.

In the acute experiment using STS on RP patients, the efficient parameters were used to maximize the efficacy of stimulation during the limited hours of an experiment. Transscleral monopolar stimulation was effective in finding the best area to create a scleral pocket for the implantation of the nine-channel electrode. The low threshold area corresponded anatomically to the macular area (just posterior to the insertion of inferior oblique muscle), which was consistent with the results of epiretinal prosthesis [7].

Localized phosphenes were elicited by the nine-channel STS system in two patients with advanced RP. Two-point discrimination (dumbbell-shaped phosphene) was also attained in the two patients, and primitive pattern recognition was obtained in patient 1. These results suggest that STS has the potential for being the basis for a pattern recognition system and be a feasible artificial vision system.

The charge densities to evoke phosphene by STS in two RP patients were 0.48 to 1.27 mC/cm2, which were comparable to the reported data of epiretinal stimulation, 0.28 to 2.88 mC/cm2 in RP patients using 400-um electrode [22].

In summary, biphasic pulses with a duration of 0.5–1.0 ms, interpulse delay of 1 ms, frequency of 20–50 Hz and trains of 10 to 20 were optimal for evoking phosphenes from localized extraocular stimulation. The STS using these parameters for advanced RP elicited localized phosphenes and enabled two-point discrimination, suggesting that STS is feasible as an approach to retinal prosthesis.

Acknowledgements The authors thank Yozo Miyake, Satoshi Suzuki, Mineo Kondo Yutaka Fukuda, Hajime Sawai and Tomomitsu Miyoshi for advice and discussion.

Commercial interest Hiroyuki Kanda and Motoki Ozawa are employees of the Nidek Company.

Financial support This study was supported by Health Sciences Research Grants (H16-sensory-001) from the Ministry of Health, Labor and Welfare, Japan.

References

1. Chow AY, Chow VY (1997) Subretinal electrical stimulation of the rabbit retina. Neurosci Lett 225:13–16
2. Chow AY, Chow VY, Packo KH, Pollack JS, Peyman GA, Schuchard R (2004) The artificial silicon retina microchip for the treatment of vision loss from retinitis pigmentosa. Arch Ophthalmol 122:460–469
3. Chowdhury V, Morley JW, Coroneo AM (2005) Stimulation of the retina with a multiekectrode extraocular visual prosthesis. ANZ J Surg 75:679–704
4. Hesse L, Schanze T, Wilms M, Eger M (2000) Implantation of retina stimulation electrodes and recording of electrical stimulation responses in the visual cortex of the cat. Graefe Arch Clin Exp Ophthalmol 238:840–845
5. Humayun MS, Price M, de Juan E Jr et al (1999) Morphometric analysis of the extramacular retina from postmortem eyes with retinitis pigmentosa. Invest Ophthalmol Vis Sci 40:143–148
6. Humayun MS, de Juan E, Weiland JD, Dagnelie G, Katona S, Greenberg R, Suzuki S (1999) Pattern electrical stimulation of human retina. Vision Res 39:2569–2576
7. Humayun MS, Weiland JD, Fujii GY, Greenberg R, Williamson R, Little J, Mech B, Cimmarusti V, Van Boemel G, Dagnelie G, de Juan E (2003) Visual perception in a blind subject with a chronic microelectronic retinal prosthesis. Vision Res 43:2573–2581
8. Jensen RJ, Rizzo JF 3rd, Ziv OR, Grumet A, Wyatt J (2003) Thresholds for activation of rabbit retinal ganglion cells with an ultrafine, extracellular microelectrode. Invest Ophthalmol Vis Sci 44:3533–3543
9. Jensen RJ, Ziv OR, Rizzo JF 3rd (2005) Thresholds for activation of rabbit retinal ganglion cells with relatively large, extreacellular microelectrodes. Invest Ophthalmol Vis Sci 46:1486–1496
10. Kanda H, Morimoto T, Fujikado T, Tano Y, Fukuda Y, Sawai H (2004) Electrophysiological studies on the feasibility of suprachoroidal-transretinal stimulation for artificial vision in normal and RCS Rat. Invest Ophthalmol Vis Sci 45:560–566

11. Kawasumi M (1981) Distribution of current intensities inside the electrically stimulated eye. Nippon Ganka Gakkai Zasshi 89:766–772
12. Leventhal AG, Rodieck RW, Dreher B (1981) Retinal ganglion cell classes in the old world monkey: morphology and central projections. Science 213:1139–1142
13. Majji AB, Humayun MS, Weiland JD, Suzuki S, D'Anna SA, de Juan E Jr (1999) Long-term histological and electrophysiological results of an inactive epiretinal electrode array implantation in dogs. Invest Ophthalmol Vis Sci 40:2073–2081
14. Margalit E, Maia M, Weiland JD, Greenberg RJ, Fujii GY, Torres G, Piyathaisere DV, O'Hearn TM, Liu W, Lazzi G, Dagnelie G, Scribner DA, de Juan E Jr, Humayun MS (2002) Retinal prosthesis for the blind. Surv Ophthalmol 47:335–356
15. Marmor MF, Aguirre G, Arden G et al (1983) Retinitis pigmentosa: a symposium on terminology and methods of examination. Ophthalmology 90:126–131
16. Miyake Y, Yanagida K, Yagasaki K (1980) Clinical application of EER (electrically evoked response) (2) Analysis of EER in patients with dysfunctional rod or cone visual pathway. Nippon Ganka Gakkai Zasshi 84:502–509
17. Morimoto T, Fukui T, Matsushita K, Okawa Y, Shimojyo H, Kusaka S, Tano Y, Fujikado T (2006) Evaluation of residual retinal function by pupillary constrictions and phosphenes using transcorneal electrical stimulation in patients with retinal degeneration. Graefe Arch Clin Exp Ophthalmol 244:1283–1292
18. Motokawa K, Ebe M (1952) Selective stimulation of color receptors with alternating currents. Science 25(115):92–94
19. Nakauchi K, Fujikado T, Kanda H, Morimoto T, Choi JS, Ikuno Y, Sakaguchi H, Kamei M, Ohji M, Yagi T, Nishimura S, Sawai H, Fukuda Y, Tano Y (2005) Transretinal electrical stimulation by an intrascleral multichannel electrode array in rabbit eyes. Graefe Arch Clin Exp Ophthalmol 243:169–174
20. Pagon RA (1988) Retinitis pigmentosa. Surv Ophthalmol 33:137–177
21. Potts AM, Inoue J (1969) The electrically evoked response of the visual system (EER) II. Effect of adaptation and retinitis pigmentosa. Invest Ophthalmol 8:605–613
22. Rizzo JF 3rd, Wyatt J, Loewenstein J, Kelly S, Shire D (2003) Method and perceptual threshold for short-term electrical stimulation of human retina with a microelectrode array. Invest Ophthalmol Vis Sci 44:5355–5361
23. Rizzo JF 3rd, Wyatt J, Loewenstein J, Kelly S, Shire D (2003) Perceptual efficacy of electrical stimulation of human retina with a microelectrode array during short-term surgical trials. Invest Ophthalmol Vis Sci 44:5362–5369
24. Santos A, Humayun MS, de Juan E Jr, Greenburg RJ, Marsh MJ, Klock IB, Milam AH (1997) Preservation of the inner retina in retinitis pigmentosa: a morphometric analysis. Arch Ophthalmol 115:511–515
25. Schwahn HN, Gekeler F, Kohler K, Kobuch K, Sachs HG, Schulmeyer F, Jakob W, Gabel VP, Zrenner E, Schwahn HN (2001) Studies on the feasibility of a subretinal visual prosthesis: data from Yucatan micropig and rabbit. Graefe Arch Clin Exp Ophthalmol 239:961–967
26. Stone J, Fukuda Y (1974) Properties of cat's retinal ganglion cells: a comparison of W-cells with X-cells and Y-cells. J Neurophysiol 37:722–748
27. Stone JL, Barlow WE, Humayun MS, de Juan E Jr, Milam AH (1992) Morphometric analysis of macular photoreceptors and ganglion cells in retinas with retinitis pigmentosa. Arch Ophthalmol 110:1634–1639
28. Tanino T, Kato S, Kawasumi M (1981) Studies on electrically evoked pupillary reflex-Indirect reflex and its frequency characteristics. Jpn J Ophthalmol 25:423–429
29. Veraart C, Raftopoulos C, Mortimer JT, Delbeke J, Pins D, Michaux G, Vanlierde A, Parrini S, Wanet-Defalque MC (1998) Visual sensations produced by optic nerve stimulation using an implanted self-sizing spiral cuff electrode. Brain Res 813:181–186
30. Walter P, Heimann K (2000) Evoked cortical potentials after electrical stimulation of the inner retina in rabbits. Graefe Arch Clin Exp Ophthalmol 238:315–318
31. Zrenner E (2002) Will retinal implants restore vision? Science 295:1022–1025

Optical Imaging to Evaluate Retinal Activation by Electrical Currents Using Suprachoroidal-Transretinal Stimulation

Yoshitaka Okawa,[1] Takashi Fujikado,[1] Tomomitsu Miyoshi,[2] Hajime Sawai,[2] Shunji Kusaka,[1] Toshifumi Mihashi,[3] Yoko Hirohara,[3] and Yasuo Tano[4]

Purpose. To determine whether reflectance changes of the retina after electrical suprachoroidal-transretinal stimulation (STS) can be detected with a newly developed optical imaging fundus camera.

Methods. Ten eyes of 10 cats were studied. A small retinal area was focally stimulated with electric currents passing between an active electrode placed in the fenestrated sclera and a reference electrode in the vitreous. Biphasic pulses were applied for 4 seconds with a current up to 500 μA. Images of the fundus illuminated with near-infrared (800–880 nm) light were obtained every 20 msec for 26 seconds between 2 seconds before and 20 seconds after the STS. Twenty images of 20 consecutive experiments were averaged. A two-dimensional map of the reflectance changes was constructed by subtracting the images before the stimulation from those after the stimulation. STS-evoked potentials (EPs) were recorded from the optic chiasma.

Results. Approximately 0.5 second after the onset of STS, reflectance changes were observed around the retinal locus, where the stimulating electrodes were positioned. The intensity of the reflectance changes was correlated with the intensity of the stimulus current. The area of the reflectance change increased as the current intensity increased and was correlated with the amplitude of the EPs ($R^2 = 0.82$).

Conclusions. Reflectance changes after STS were localized to the area around the electrode. The strong correlation between the area of the reflectance changes and the amplitude of the EPs suggested that the reflectance changes reflected the activity of retinal neurons elicited by electrical stimulation. (*Invest Ophthalmol Vis Sci.* 2007;48: 4777–4784) DOI:10.1167/iovs.07-0209

From the Departments of [1]Applied Visual Science, [2]Physiology, and [4]Ophthalmology, Osaka University Graduate School of Medicine, Suita, Japan; and [3]Topcon Research Institute, Itabashi, Japan.

Supported by Health Sciences Research Grants (H16-sensory-001) from the Ministry of Health, Labor and Welfare, Japan and by Grant 18591918 from the Ministry of Education, Culture, Science and Technology.

Submitted for publication February 18, 2007; revised May 21, 2007; accepted August 10, 2007.

Disclosure: **Y. Okawa**, None; **T. Fujikado**, None; **T. Miyoshi**, None; **H. Sawai**, None; **S. Kusaka**, None; **T. Mihashi**, Topcon Research Institute (E); **Y. Hirohara**, Topcon Research Institute (E); **Y. Tano**, None

The publication costs of this article were defrayed in part by page charge payment. This article must therefore be marked "*advertisement*" in accordance with 18 U.S.C. §1734 solely to indicate this fact.

Corresponding author: Takashi Fujikado, Department of Applied Visual Science, Osaka University Graduate School of Medicine, 2-2 Yamadaoka, Suita, Osaka 565-0871, Japan; fujikado@ophthal.med.osaka-u.ac.jp.

In vivo optical imaging of intrinsic signals is a well-established method to study brain physiology and to map the functional architecture of the cerebral cortex.[1–4] In optical imaging studies, stimulus-induced neuronal activity is detected as a change of light reflectance. The reflectance change does not directly indicate neural activation, but it is strongly correlated with the activity of neurons examined by conventional extracellular recordings.[5] Studies of cortical optical imaging have shown that this intrinsic signal originates from stimulus-induced changes in the light-scattering of neural tissues and from changes in light absorption associated with hemodynamic changes in blood volume or the oxygenated state of hemoglobin.[6,7]

Recently, the technique of optical imaging has been applied to the retina to examine light-evoked reflectance changes.[8–10] Although the light-evoked neuronal activity in localized areas of the retina can be recorded by multifocal electroretinography (mfERG),[11] those evoked by electrical stimulation are difficult to detect by mfERG because of the large stimulus artifact. Therefore, optical recording is a reasonable alternative to study the responses evoked by the electrical stimulation of the retina.

Artificial retinas, also called retinal prostheses, have been placed at different sites.[12–15] A typical retinal prosthesis consists of an array of electrodes implanted above (epi-) or beneath (sub-) the retina and is used to deliver electrical current to the retina to evoke a light sensation called a phosphene. We have implanted an electrode array in the suprachoroidal space, and stimulation by this system has been called suprachoroidal-transretinal stimulation (STS).[16] In STS, the active electrode array is placed in the fenestrated sclera in the retrobulbar space while the reference electrode is inserted into the vitreous cavity. STS is a safe method and avoids the direct contact of electrodes with the retina, but the distance between electrodes and retina is larger than in the epiretinal or subretinal methods. Thus, it is necessary to determine whether sufficient spatial resolution can be achieved by this approach.

The spatial resolution of epiretinal electrodes has been investigated by optical imaging in the visual cortex[17] but not in the retina. The purpose of this study was to determine whether reflectance changes can be detected in the area of the retina activated by STS. To accomplish this, we have developed a prototype optical-imaging fundus camera to measure the changes of light reflectance evoked by electrical stimulation of the retina.

Materials and Methods

Animals

Ten left eyes of 10 cats under general anesthesia were used. Cat 1 was used for the study of light stimulation, and cats 2 through 10 were used for the electrical stimulation. Cats 6, 7, and 9 were also used for the study of evoked potential (EP) at optic chiasm. Initially, each animal received an intramuscular injection of ketamine hydrochloride (25

mg/kg) and an intraperitoneal injection of atropine sulfate (0.1 mg/kg). Then each animal was anesthetized by intravenous infusion of pentobarbital sodium (1 mg/kg per hour) and paralyzed by pancuronium bromide (0.2 mg/kg per hour) mixed with Ringer solution and glucose (0.1 g/kg per hour).

The animal was artificially ventilated with a mixture of N_2O/O_2 (1:1), and the end-tidal CO_2 concentration was controlled at 3.5% to 5.0% by altering the frequency and volume of ventilation. In addition to the continuous monitoring of the expired CO_2, the intratracheal pressure and electrocardiogram were also monitored. Body temperature was maintained with a heating pad at 38°C.

Surgical Procedures

An incision was made over the temporal area of the left eye; part of the lateral orbital wall (zygomatic and frontal bone) was removed, and the lateral rectus muscle was dissected. The scleral area just above the long ciliary artery was exposed, and a 3- to 4-mm incision was made through the sclera. The conjunctiva was sutured to a fixed frame attached to the stereotaxic headholder to prevent eye movements. The pupil was dilated with 5% phenylephrine hydrochloride, 0.5% tropicamide, and 1% atropine sulfate. To protect the corneal surface, a hard contact lens was placed on the cornea (polymethylmethacrylate; base curve, 8.50 mm; power, +1.5 D; diameter, 13.5 mm). All experiments were performed in accordance with the ARVO Statement for the Use of Animals in Ophthalmic and Visual Research, and the procedures were approved by the Animal Research Committee of Osaka University Medical School.

Optical Imaging of Retina

The ocular fundus was monitored by a fundus camera (TRC-50LX; Topcon Corp., Tokyo, Japan) with a digital CCD camera (C8484; Hamamatsu Photonics, Hamamatsu, Japan). The number of pixels was 1280 × 1024, but the binning mode of the camera was used to obtain maximum light sensitivity and the resolution was reduced to 320 × 256 pixels (12-bit grayscale). A 12-bit digitizer was used, and the 4096 grayscale levels were obtained for each pixel.

A halogen lamp was used to illuminate the posterior fundus, and a bandpass filter was inserted in the illumination optical path to limit the wavelength of the fundus monitoring light between 800 and 880 nm. The power of the illuminating light was 250 nW, which was much lower than the safe exposure limit decided by American National Standard Institute.

To improve the signal-to-noise ratio, 20 images of 20 consecutive experiments were averaged (Fig. 1). The interval between each session was 1 minute. A two-dimensional image of the optical signal was obtained by subtracting the image recorded before stimulation from those after stimulation. All experiments were performed in a dark room after 30 minutes of dark adaptation.

Electrophysiological Recording from Optic Chiasma

To record the potentials evoked by electrical stimulation of the retina from the optic chiasma (OX), a pair of stainless steel electrodes was placed in the OX stereotaxically. Light-evoked responses were recorded from each electrode to be certain that the electrodes were placed in the OX.

To record the electrically evoked potentials (EEPs), the signal was amplified 10,000 times and was bandpass filtered between 300 Hz and 5 kHz with an AC amplifier (model 1800; Microelectrode AC amplifier; A-M Systems, Inc., Carlsborg, WA) and a signal conditioner (LPF-202A; Warner Instruments, Hamden, CT). Amplified EEPs were fed to a signal processor (Power 1401; Cambridge Electronic Design, Cambridge, UK) with a sampling frequency of 50 kHz and were analyzed off-line. Signals were also monitored on an oscilloscope and an audio speaker in real time.

Focal Light Stimulation of Retina

The stimuli were obtained from white light-emitting diodes controlled by a pulse generator. The stimulating light was a vertical bar focused on the retina, flickering at 8 Hz for 4 seconds. The width of the bar was 4°, and the center of the bar was located 6° temporal to the fovea (Fig. 2A). The light power was 30 nW. Images were obtained every 20 msec for 18 seconds between 2 seconds before and 12 seconds after the stimulus.

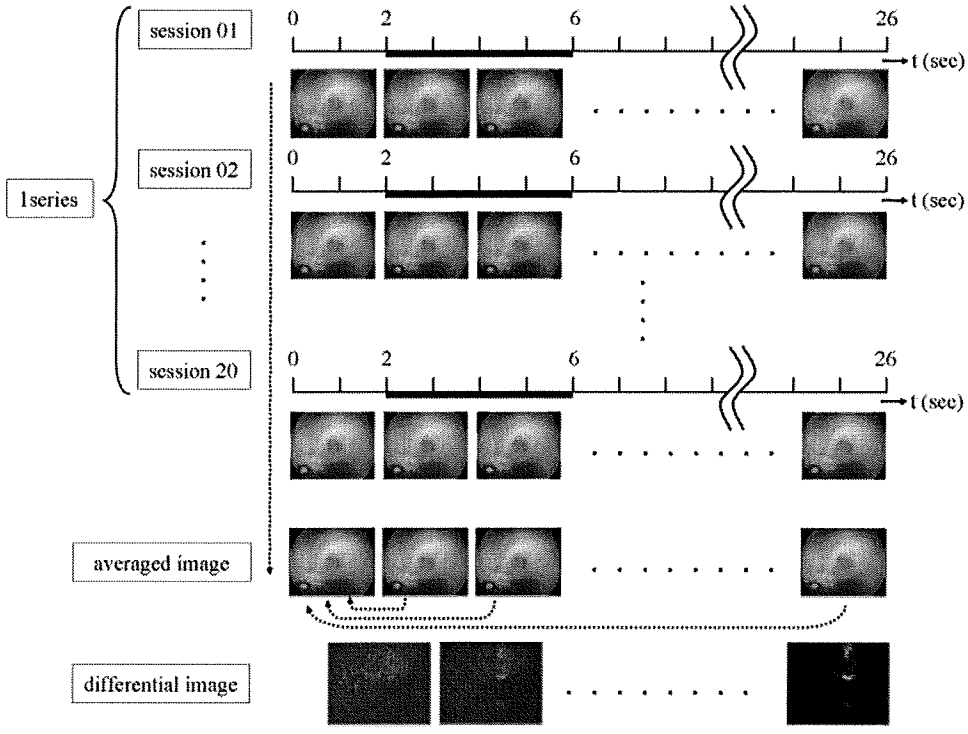

FIGURE 1. Sequence of image processing for optical imaging in this experiment.

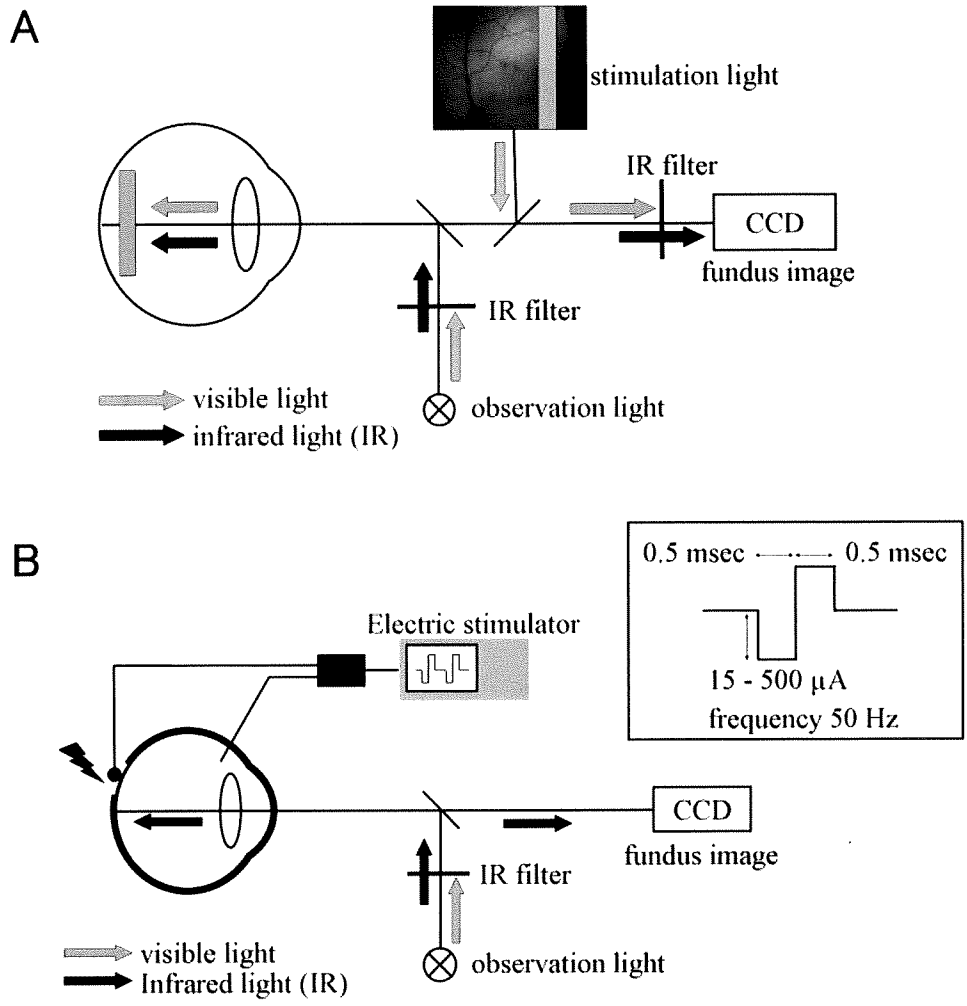

FIGURE 2. Schema of optical imaging for light stimulation (**A**) and for STS (**B**).

Focal Electrical Stimulation of Retina

A single-channel platinum electrode (diameter, 100 μm) was used as the active scleral electrode. A vitreous electrode was inserted into the vitreous through the sclera at the pars plana. This electrode was a urethane-coated platinum wire (0.2 mm in diameter), and its exposed tip measured approximately 2 mm. The active electrode was held gently against the sclera by a manipulator, and the pressure on the eye was minimal, as determined by the degree of indentation of the retina viewed by the fundus camera. The mass EP at the OX elicited by STS was also monitored to confirm the effectiveness of the electrical stimulation.

For each STS trial, biphasic pulse trains (outward first) were applied at 50-Hz frequency, 0.5-msec pulse duration, and 4-second stimulation (Fig. 2B). All pulses were generated by a pulse generator (SEN7203; Nihon Kohden Corp., Tokyo, Japan) and were delivered to the electrodes through a linear stimulus isolation unit (BSI-950; Dagan Corporation, Minneapolis, MN).

To evaluate the correlation between the stimulus current and the area of reflectance change, the stimulating current was increased systematically between the threshold current to the maximum current (≤500 mA) or decreased systematically to examine hysteresis. Images were obtained every 20 msec for 26 seconds between 2 seconds before and 20 seconds after the electrical stimulation.

Data Analyses

Optical Density Measurements. To evaluate the intensity of the reflectance, the grayscale value (GSV) of each spot in the focused area was averaged. The averaged GSV of each spot after the onset of light or electrical stimulation was subtracted from that before the electrical stimulation to obtain the differential image (Fig. 1). For the evaluation of the area of reflectance change, the GSV value of 40 (approximately 8 SD of the GSV without stimulation) was set as the cutoff level to reduce the effect of baseline fluctuations. To study the relationship between the area of reflectance change (pixels) and the stimulus current, the maximum number of pixels in which the averaged reflectance change exceeded the cutoff level (±40 GSV) during the time course was selected to determine the maximum area of reflectance change. The number of pixels with an increase or a decrease of reflectance was added to evaluate the area of retinal excitation.

Electrophysiological Measurements. The amplitude of the EPs evoked by STS was determined by measuring the amplitude between the first negative peak (latency approximately 3.0 msec) and the second positive peak (latency approximately 4.0 msec). Two hundred records were averaged to determine the amplitude for a particular stimulus current.

Statistical Analysis

Regression analysis between the stimulus current and the area of reflectance change or the amplitude of EP at OX was evaluated by SPSS (SPSS Inc., Chicago, IL).

RESULTS

Optical Imaging after Light Stimulation

Examination of a two-dimensional map of the reflectance changes after light stimulation showed that the reflectance

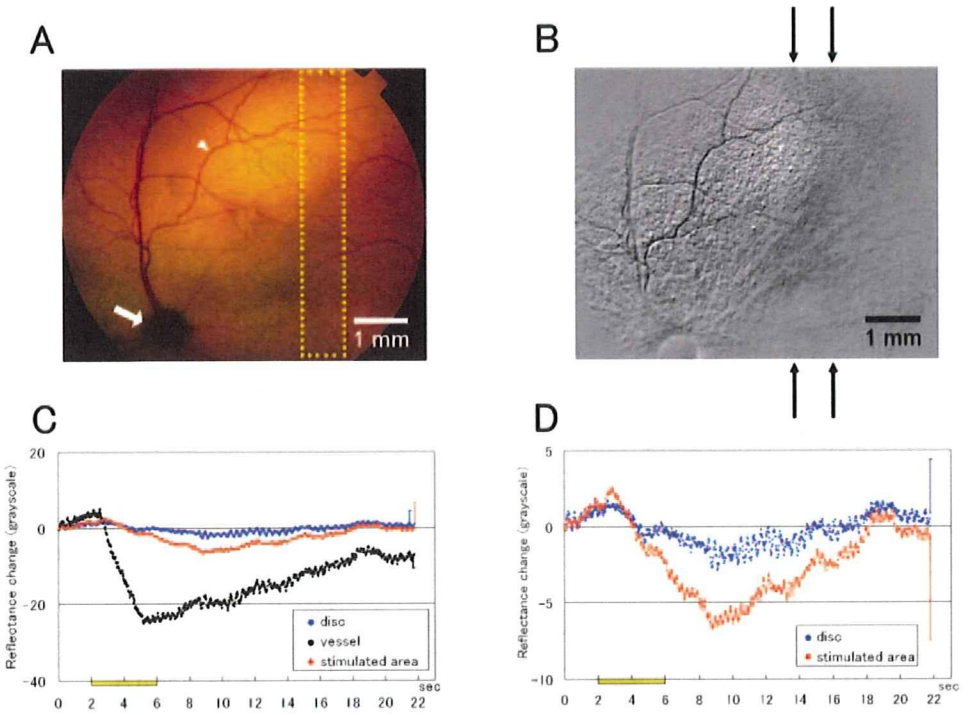

FIGURE 3. Results of optical imaging for light stimulation. **(A)** Color fundus photograph of cat retina. **(B)** Two-dimensional map of reflectance changes (differential map) 3 seconds after the onset of light stimulation. *Black arrows*: area of light stimulation. **(C)** Changes of light reflectance at the blood vessel (*black line*), at optic disc (*blue line*), and at stimulated retinal area (*red line*). **(D)** Magnified image of **(C)**. **(A)** Area of reflectance change measured for the blood vessel (*arrowhead*), optic disc (*arrow*), and retina (*yellow dots*). **(C, D)** *Yellow bar*: period of light stimulation. **(A, B)** *Bars*: scale of ocular fundus. **(C, D)** *Bars*: SD of reflectance change.

decreased in the stimulated striped area (Fig. 3). Reflectance of the retinal vessels began to decrease approximately 0.5 second after the stimulus onset and continued to decrease linearly to a deep trough at approximately 3.5 seconds (Fig. 3C). The change of reflectance of the optic disc and stimulated retinal area showed similar temporal changes. Reflectance began to decrease approximately 1.0 second after the stimulus onset and continued to decrease almost linearly to a deep trough at approximately 7.0 seconds after the stimulus onset (Fig. 3D).

Optical Imaging of STS

A two-dimensional map of the reflectance changes after electrical stimulation showed an increase of reflectance in the retinal area, where the tip of the electrode was attached to the sclera. A decrease of reflectance was observed in the retinal area surrounding the area of increased reflectance (Fig. 4; see also Fig. 7A). The time course of the reflectance changes was similar with the different intensities of electrical stimulation.

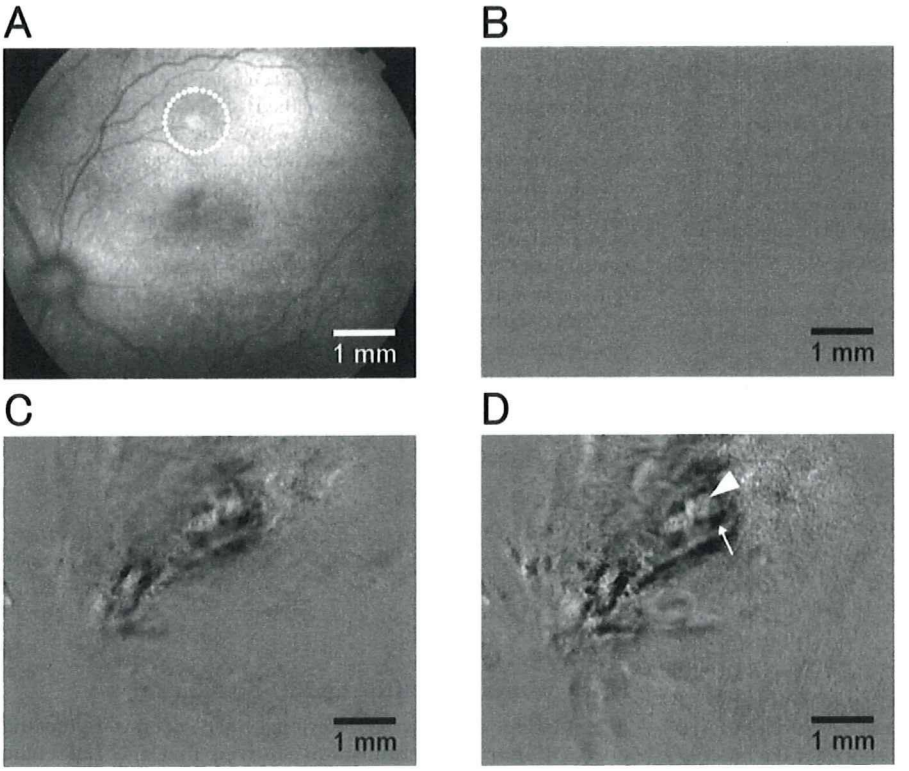

FIGURE 4. Results of optical imaging for electrical stimulation. **(A)** Fundus photograph of a cat retina with an electrode attached to the hemidissected sclera. *Dotted white circle*: position of the electrode. **(B–D)** Differential map of the reflectance change 2 seconds after the onset of electrical stimulation. **(B)** No stimulation. **(C)** Stimulus current of 125 μA. **(D)** Stimulus current of 250 μA. *Arrowhead*: high-reflectance area at the electrode. *Arrow*: low-reflectance area surrounding the electrode. **(A–D)** *Bars*: scale of ocular fundus.

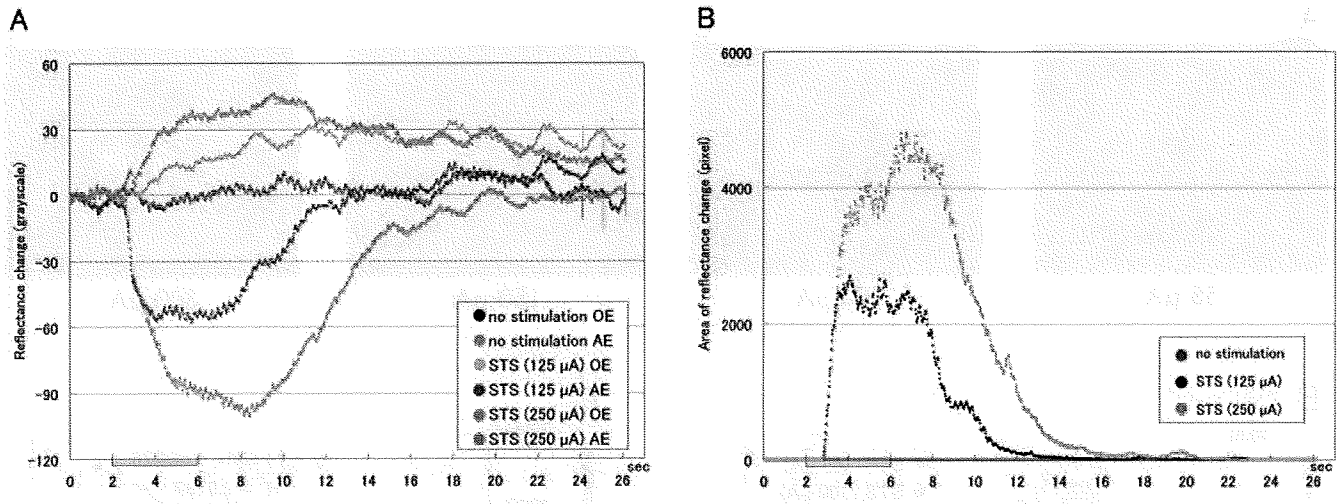

FIGURE 5. Time course of the intensity of reflectance change (**A**) and the area of reflectance change (**B**) in cat 2. (**A**) Intensity (gray scale) of reflectance change with currents of (*red line*) 250 μA and (*dark blue line*) 125 μA around the electrode (AE). Reflectance change with currents of (*purple line*) 250 μA and (*light blue line*) 125 μA on the electrode (OE). *Black line*: reflectance change OE without electrical stimulation. *Bar*: SD of reflectance change. (**B**) Area (pixels) of reflectance change with currents of (*red line*) 250 μA and (*black line*) 125 μA and with (*blue line*) no stimulation.

The increase at the electrode or the decrease surrounding the electrode of light reflectance was observed approximately 0.5 second after the stimulus onset, increased or decreased rapidly for 1.5 to 2.0 seconds, increased or decreased gradually to peak at 4 to 6 seconds after stimulus onset, and then returned to the baseline gradually (Figs. 5A, 6A). Reflectance did not change at the electrode site when stimulation was not applied (Fig. 5A). The maximum value of reflectance increase on the electrode or reflectance decrease around the electrode was linearly related to the increase of stimulus intensity (Fig. 6B).

The area of the reflectance change (increased and decreased reflectance areas were combined) had a similar time course with different stimulus intensities. The area began to increase approximately 0.5 second to 1.0 second after stimulus onset and changed linearly for 1.0 to 1.5 seconds The size of the area peaked 2 to 5 seconds after stimulus onset, was sustained for 4 to 8 seconds, and returned to the baseline gradually (Figs. 5B, 7B). The area of the reflectance changes increased with an increase of current intensity (Fig. 7C). Reflectance changes on and around the electrode were not observed when stimulation was not applied (Fig. 5B).

The threshold current for eliciting a reflectance change ranged from 65 μA to 200 μA for the different cats. Linear regression analysis showed that R^2 ranged from 0.82 to 0.97 in the 9 cats (cats 2–10), suggesting that the area of reflectance changed linearly with the stimulus current intensity. The slope of the regression line varied in the different cats (Fig. 8).

Electrophysiological Recordings from Optic Chiasm after STS

We examined the relationship between the EP amplitude recorded in the OX and the stimulus current in three cats (cats 6, 7, 9; Fig. 9). EP amplitude increased linearly with an increase of stimulus current (Fig. 10). Linear regression analysis showed the R^2 values were 0.89, 0.95, and 0.98, respectively, suggest-

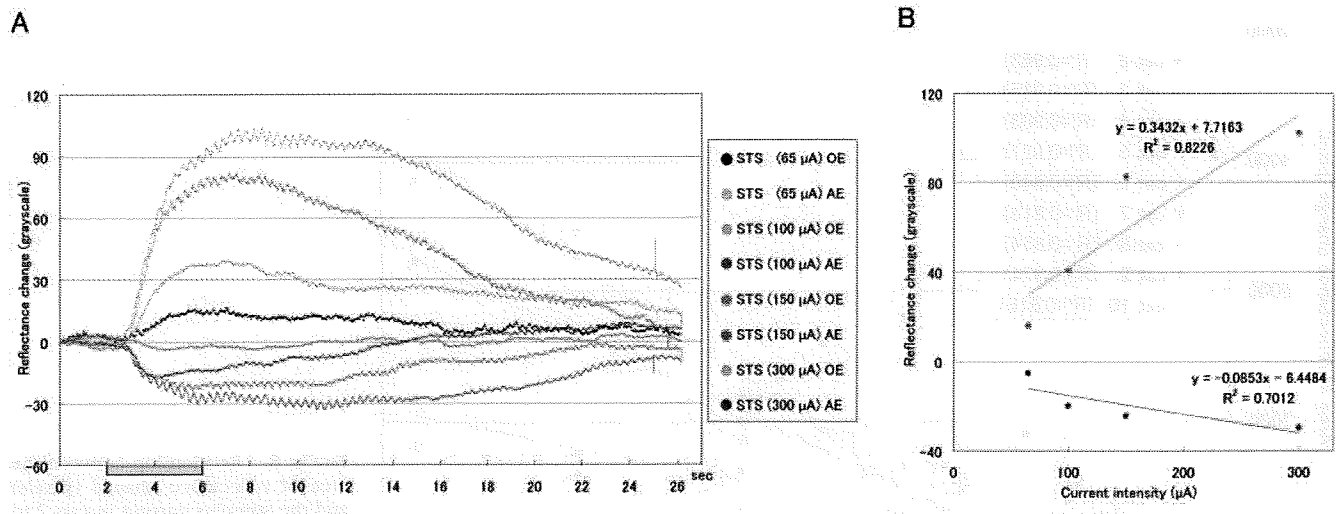

FIGURE 6. Time course of the reflectance change in cat 3. (**A**) Time course of the intensity of reflectance change. (**B**) Relationship between the maximum intensity of reflectance change and the stimulus current. (**A**) Reflectance change with currents of (*green line*) 300 μA, (*purple line*) 150 μA, (*light blue line*) 100 μA, and (*black line*) 65 μA on electrodes. Reflectance change with currents of (*dark green line*) 300 μA, (*red line*) 150 μA, (*dark blue line*) 100 μA, (*gray line*) and 65 μA around electrodes. (**B**) Linear regression line of maximum reflectance change (*red line*) on the electrode and (*blue line*) around the electrode. (**A**) *Bar*: SD of reflectance change.

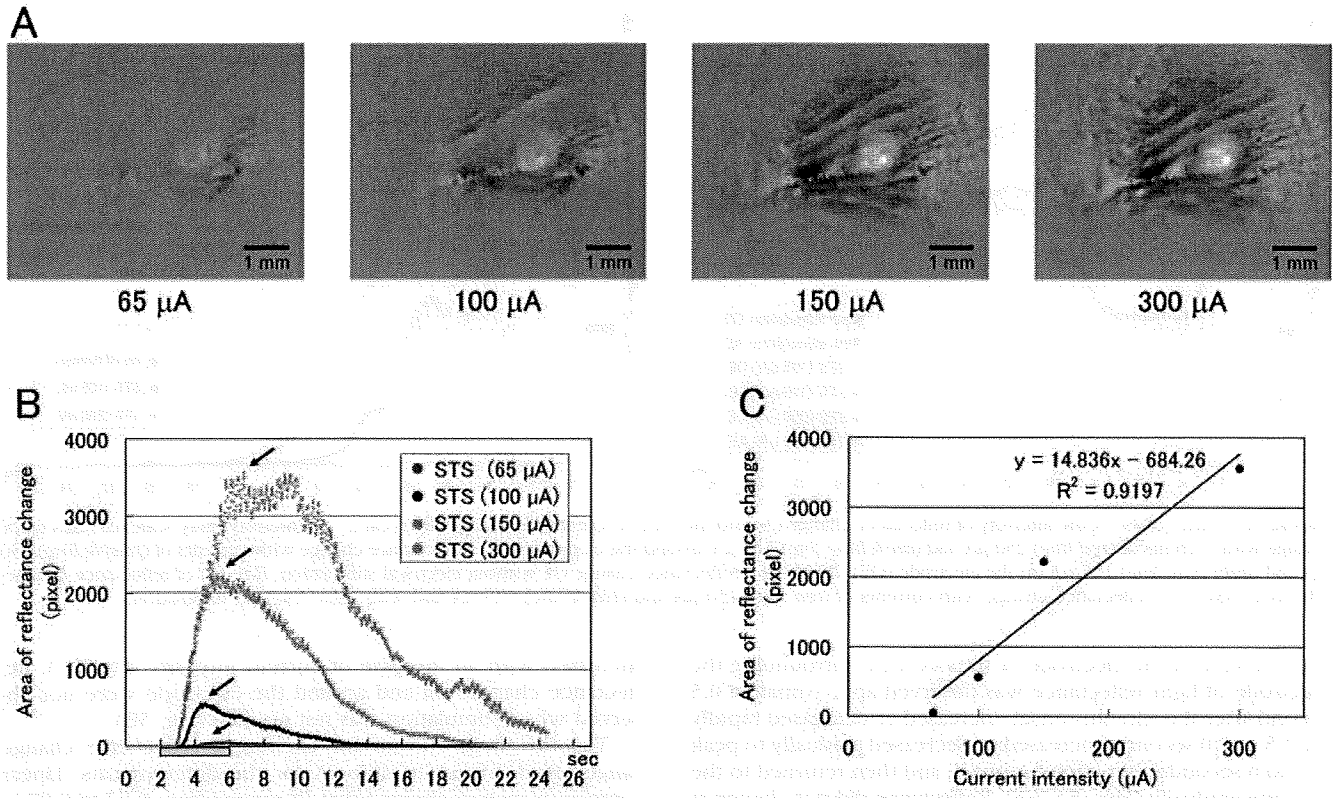

FIGURE 7. The area of reflectance change in relation to the electrical current in cat 3. (A) Differential image of the reflectance changes of the retina 2.4 seconds after the onset of electrical stimulation with an electrical current from 65 μA to 300 μA. (B) Time course of the area (pixels) of reflectance change with different stimulus currents. *Purple*, 300 μA; *red*, 150 μA; *black*, 100 μA; *blue*, 65 μA. (C) Relationship between the maximum area of reflectance change (pixels) and the stimulus current. (A) *Bars*: scale of ocular fundus.

ing that the EP changed linearly with the stimulus current intensity. The slope of the regression line varied in the different cats (data are not shown).

The relationship between the amplitude of EP and the area of reflectance change was also assessed in cats 6, 7, and 9. Linear regression analysis showed that the R^2 values were 0.82, 0.84, and 0.82, respectively, suggesting that the reflectance changed linearly with the EP at OX through electrical stimulation to the retina (Fig. 10).

DISCUSSION

We have developed an optical imaging system to evaluate the retinal area activated by focal electrical stimulation to the

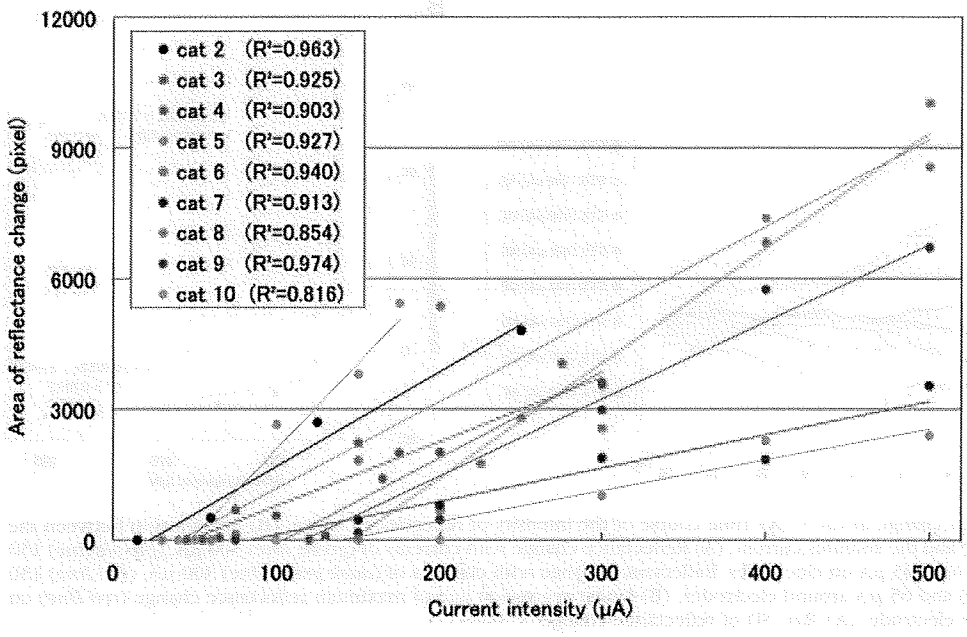

FIGURE 8. Relationship between the area of reflectance change (pixels) and the stimulus current in cats 2 to 10. Each point represents the maximum number of pixels during or after electrical stimulation in which the reflectance change exceeded the cutoff level (gray scale value of 40).

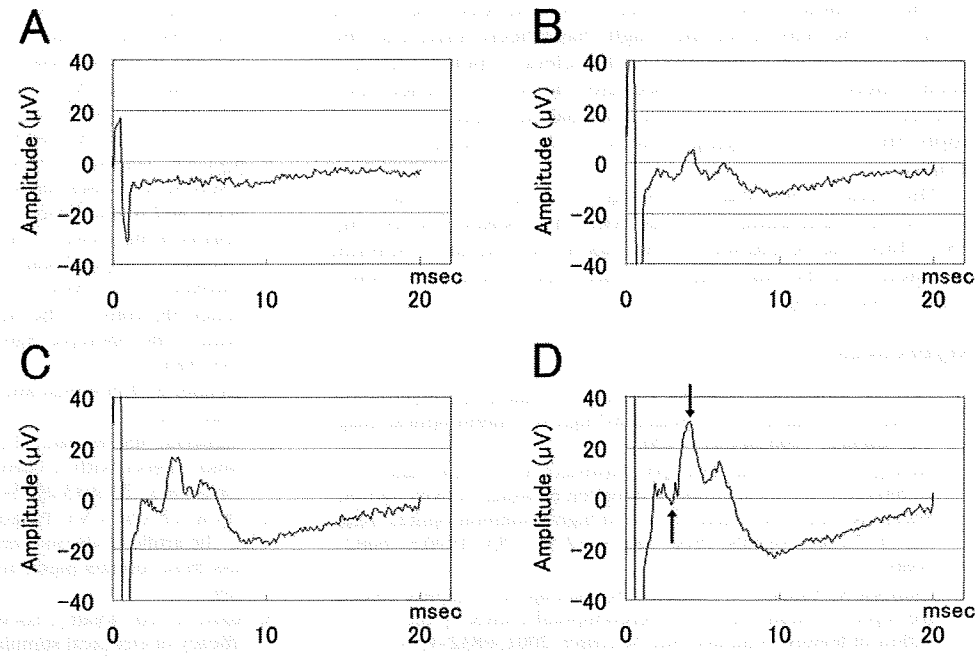

FIGURE 9. Example of EP recorded in optic chiasma in response to STS with currents of 60 μA (A), 150 μA (B), 300 μA (C), and 500 μA (D) in cat 7. (D) *Arrows*: first negative peak and second positive peak. EP amplitude was evaluated between these peaks.

retina. To confirm that our system measured the retinal area in which the retina was activated, we examined whether the reflectance of infrared light changed in response to flickering visible light stimulation. Our results showed that a decrease in reflectance in the area corresponded with the light-stimulated striped area (Fig. 3), as reported by Ts'o et al. for light stimulation (Ts'o D, et al. *IOVS* 2004;45:ARVO E-Abstract 3495). Tsunoda et al.[8] also reported decreased light reflectance that peaked within 1 second of light stimulation, faster than our observation (peak approximately 7 seconds; Fig. 3). This discrepancy might have occurred because we used continuous flickering light whereas Tsunoda et al.[8] used single-flashed light. Indeed, the time course of the reflectance change in our case was similar to that of Ts'o D, et al. (*IOVS* 2004;45:ARVO E-abstract 3495) who used flickering light.

With focal electrical stimulation, the reflectance increased or decreased depending on the retinal area (Fig. 4). Reflectance changes induced by electrical stimulation had fast and slow phases, whereas those induced by light stimulation were monotonic, suggesting that the time course to activate the retina that induced the reflectance changes was different by light stimulation than it was by electrical stimulation (Figs. 3–6).

The origin of the positive change of reflection is a matter of discussion, but, because the time course of positive and negative reflection changes were similar, we suggest that both positive and negative reflection changes were evoked by the same mechanism related to the retinal activation (Figs. 5, 6). Therefore, we added the absolute value of positive and negative reflectance change as a parameter of reflectance changes.

The change in reflectance intensity was linearly related to the intensity of the electrical current (Fig. 6). If we consider that the change in reflectance was correlated with the local retinal response,[8] the value of the reflectance change might have reflected the degree of retinal activation induced by the electrical current. The area of the reflectance change was correlated with the simulating current, suggesting that the area of reflectance change represented the area of the retina activated by electrical stimulation (Fig. 8). This supports the results of electrophysiological studies showing that the area of retinal excitation was correlated with the intensity of electrical current (Kanda H, et al. *IOVS* 2005;46:ARVO E-Abstract 1499).

In the electrophysiological data from the OX, the maximum amplitude of the EP was strongly correlated with the intensity of stimulus current (Fig. 10), suggesting that focal electrical stimulation in the retina activated retinal ganglion cells (RGCs) in proportion to the intensity of stimulation current. EP amplitude was correlated with the total pixels of reflectance change in the retina, suggesting that the area of reflectance change represented neuronal changes in the retina, which led to the excitation of the RGCs.

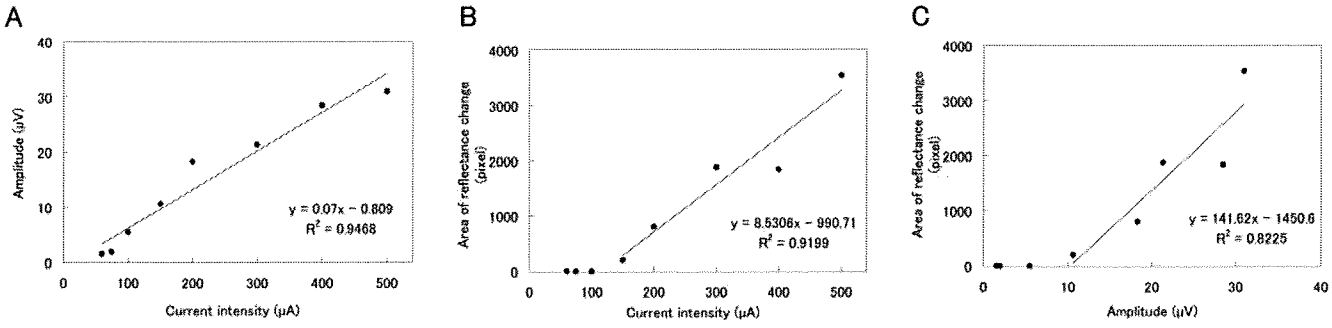

FIGURE 10. Relationships between EP amplitude and stimulus intensity (A), area and stimulus intensity (B), and area and EP amplitude in cat 7 (C).

The threshold current of retinal activation was different for each cat. The reason for this might have been related to the degree of electrode connection to the sclera, which could have been different in each cat. Because the area of reflectance change was correlated with the stimulating current, we may apply this optical imaging system to the artificial retina in humans.

The area of reflectance change is confined to the area around the stimulating electrode with threshold currents (Fig. 7A). Thus, the resolution of the electrode and the optimum parameter for the stimulation of each electrode can be determined objectively.

References

1. Ts'o DY, Frostig RD, Lieke EE, Grinvald A. Functional organization of primate visual cortex revealed by high resolution optical imaging. *Science*. 1990;249:417-420.
2. Frostig RD, Lieke EE, Ts'o DY, Grinvald A. Cortical functional architecture and local coupling between neuronal activity and the microcirculation revealed by in vivo high-resolution optical imaging of intrinsic signals. *Proc Natl Acad Sci USA*. 1990;87:6082-6086.
3. Tsunoda K, Yamane Y, Nishizaki M, Tanifuji M. Complex objects are represented in macaque inferotemporal cortex by the combination of feature columns. *Nat Neurosci*. 2001;4:832-838.
4. Taga G, Asakawa K, Maki A, Konishi Y, Koizumi H. Brain imaging in awake infants by near-infrared optical tomography. *Proc Natl Acad Sci USA*. 2003;100:10722-70727.
5. Das A, Gilbert CD. Long-range horizontal connections and their role in cortical reorganization revealed by optical recording of cat primary visual cortex. *Nature*. 1995;375:780-784.
6. Cohen LB. Changes in neuron structure during action potential propagation and synaptic transmission. *Physiol Rev*. 1973;53:373-418.
7. Holthoff K, Writte OW. Intrinsic optical signals in rat neocortical slices measured with near-infrared dark-field microscopy reveal changes in extracellular space. *J Neurosci*. 1996;16:2740-2749.
8. Tsunoda K, Oguchi Y, Hanazono G, Tanifuji M. Mapping cone- and rod- induced retinal responsiveness in macaque retina by optical imaging. *Invest Ophthalmol Vis Sci*. 2004;45:3820-3826.
9. Riva CE, Logean E, Falsini B. Visually evoked hemodynamical response and assessment of neurovascular coupling in the optic nerve and retina. *Prog Retin Eye Res*. 2005;24:183-215.
10. Abramoff MD, Kwon YH, Ts'o D, et al. Visual stimulus-induced changes in human near-infrared fundus reflectance. *Invest Ophthalmol Vis Sci*. 2006;47:715-721.
11. Sutter EE, Tran D. The field topography of ERG components in man, I: the photopic luminance response. *Vision Res*. 1992;32:433-446.
12. Zrenner E. Will retinal implants restore vision? *Science*. 2002;295:1022-1025.
13. Humayun MS, Weiland JD, Fujii GY, et al. Visual perception in a blind subject with a chronic microelectronic retinal prosthesis. *Vision Res*. 2003;43:2573-2581.
14. Chow AY, Chow VY, Packo KH, Pollack JS, Peyman GA, Schuchard R. The artificial silicon retina microchip for the treatment of vision loss from retinitis pigmentosa. *Arch Ophthalmol*. 2004;122:460-469.
15. Rizzo JF 3rd, Wyatt J, Loewenstein J, Kelly S, Shire D. Perceptual efficacy of electrical stimulation of human retina with a microelectrode array during short-term surgical trials. *Invest Ophthalmol Vis Sci*. 2003;44:5362-5369.
16. Kanda H, Morimoto T, Fujikado T, Tano Y, Fukuda Y, Sawai H. Electrophysiological studies on the feasibility of suprachoroidal-transretinal stimulation for artificial vision in normal and RCS Rat. *Invest Ophthalmol Vis Sci*. 2004;45:560-566.
17. Eckhorn R, Wilms M, Schanze T, et al. Visual resolution with retinal implants estimated from recordings in cat visual cortex. *Vision Res*. 2006;46:2675-2690.

Direct Effect of Electrical Stimulation on Induction of Brain-Derived Neurotrophic Factor from Cultured Retinal Müller Cells

Tatsuhiko Sato,[1] *Takashi Fujikado,*[1] *Tong-Sheng Lee,*[1] *and Yasuo Tano*[2]

Purpose. To investigate the direct effect of electrical stimulation (ES) on the induction of brain-derived neurotrophic factor (BDNF) from cultured retinal Müller cells.

Methods. Müller cells were isolated from rat retinas. ES was applied to passage 1 Müller cells with biphasic pulses (duration, 1 ms; frequency, 20 Hz; current, 10 mA) for 30 minutes. The changes in gene expression after ES were analyzed with microarrays. The mRNA and protein levels of BDNF were determined at each time point after ES by RT-PCR and ELISA, respectively. RT-PCR was also performed at 3 hours after ES of Müller cells that had been exposed to 1 μM nifedipine, a blocker of L-type voltage-dependent calcium channels (L-VDCCs).

Results. Microarray analyses showed an upregulation of 245 genes, including BDNF. The mRNA level of BDNF increased significantly ($P < 0.05$; by ~1.2-fold over that of the control) at 2 and 3 hours after ES. The intracellular protein level was upregulated significantly (by ~1.4-fold) at 6 hours after ES, whereas the extracellular level did not change at any time point. The total protein level of BDNF increased significantly (~1.3-fold) at 6 hours after ES. The increase in the mRNA level of BDNF was fully suppressed by exposure of the Müller cells to nifedipine.

Conclusions. These results demonstrate that ES directly upregulates the transcriptional induction of BDNF through L-VDCCs in cultured Müller cells. The ES of Müller cells may be used to supply endogenous BDNF to the retina. (*Invest Ophthalmol Vis Sci.* 2008;49:4641–4646) DOI:10.1167/iovs.08-2049

Müller cells, the predominant glial element in the retina, are believed to play important roles in maintaining its integrity and function. For example, Müller cells have been shown to express glutamate transporters,[1] which are postulated to contribute to the clearance of glutamate and protect retinal ganglion cells (RGCs) from glutamate neurotoxicity.[2–5] Müller cells also synthesize glutamine synthetase[6] which amidates glutamate to form the non-neuroactive compound glutamine.[7] In addition, Müller cells produce various neurotrophic factors, including brain-derived neurotrophic factor (BDNF),[8,9] basic fibroblast growth factor (bFGF or FGF-2),[10,11] and insulin-like growth factor (IGF)-1,[12] in reaction to different in vivo and in vitro conditions.

We have demonstrated that electrical stimulation (ES) induces the transcription of IGF-1 from cultured Müller cells and that the induction was dependent on calcium (Ca^{2+}) influx through L-type voltage-dependent calcium channels (L-VDCCs).[13] Ca^{2+} ions are the most widely used second messengers, and many of the processes that occur in the central nervous system (CNS; e.g., gene transcription), are controlled by Ca^{2+} influx.[14] For example, Ou and Gean[15] showed that the Ca^{2+} influx through *N*-methyl-D-aspartate (NMDA) receptors and L-VDCCs upregulated the transcription of BDNF in the amygdala. Sasaki et al.[16] demonstrated that Ca^{2+} entry into cortical neurons through L-VDCCs induced neuronal nitric oxide synthase (nNOS) message as well as protein synthesis. On the other hand, ES has been reported to induce different gene expressions (e.g., BDNF,[17,18] bFGF,[18] and growth-associated protein [GAP]-43[19] in both central and peripheral neurons. In addition, ES has been demonstrated to induce expression of various genes by Ca^{2+} influx through VDCCs in neurons other than those of the retina.[20,21]

Thus, we hypothesized that the Ca^{2+} influx into Müller cells via L-VDCCs that is induced by ES increases the gene expression of neurotrophic factors. To test this hypothesis, we initially performed microarray analyses to evaluate the changes in gene expression with and without ES in cultured Müller cells. Our results showed that the mRNA of BDNF was upregulated, and the time course of BDNF expression at both the message and protein levels was determined.

Materials and Methods

All experimental procedures were performed in accordance with the ARVO Statement for the Use of Animals in Ophthalmic and Vision Research and were approved by the Animal Research Committee, Osaka University Medical School.

Müller Cell Cultures

Müller cells were obtained by a method that isolates cells that were >95% pure Müller cells.[13,22] Briefly, eye cups from Long-Evans rats at postnatal days 12 to 14 were soaked in Dulbecco's modified Eagle's medium (DMEM; Nikken Biomedical Laboratory, Kyoto, Japan) supplemented with 1:1000 penicillin/streptomycin (Invitrogen Japan, Tokyo, Japan) overnight at room temperature in the dark. The eye cups were then incubated in DMEM containing 0.05% trypsin/EDTA (Invitrogen Japan) and 70 U/mL collagenase (Sigma-Aldrich, Tokyo, Japan) for 30 minutes at 37°C. The retinas were dissociated into small aggregates with a narrow-bore Pasteur pipette in culture medium. The culture medium was low-glucose DMEM supplemented with 10% fetal bovine serum (Invitrogen Japan) and 1:1000 penicillin-streptomycin. The cells were seeded into culture dishes and maintained at 37°C in a humidified atmosphere of 5% CO_2 and 95% air. When the primary cells proliferated to 80% to 90% confluence, the cells were passaged with Dulbecco's phosphate-buffered saline (DPBS; Nikken Biomedical Laboratory) supplemented with 0.05% trypsin/EDTA. The cells were seeded at the same concentration into 35-mm dishes in 2 mL fresh culture medium.

From the Departments of [1]Applied Visual Science and [2]Ophthalmology, Osaka University Medical School, Osaka, Japan.

Supported by Health Sciences Research Grant H16-sensory-001 from the Ministry of Health, Labor, and Welfare, Japan, and by Grant 18591918 from the Ministry of Education, Culture, Science, and Technology.

Submitted for publication March 19, 2008; revised April 23 and May 20, 2008; accepted August 8, 2008.

Disclosure: **T. Sato**, None; **T. Fujikado**, None; **T.-S. Lee**, None; **Y. Tano**, None

The publication costs of this article were defrayed in part by page charge payment. This article must therefore be marked "*advertisement*" in accordance with 18 U.S.C. §1734 solely to indicate this fact.

Corresponding author: Takashi Fujikado, Department of Applied Visual Science, Osaka University Medical School, 2-2 Yamadaoka, Suita, Osaka 565-0871, Japan; fujikado@ophthal.med.osaka-u.ac.jp.

Cells of passage 1, which were cultured strictly for the same period to subconfluent condition, were used in all experiments for the statistical analyses.

Conditions of ES

ES was applied to Müller cells on a clean bench.[13] Briefly, silver/silver chloride needle-type electrodes (ϕ = 0.2 mm) were inserted into culture medium without touching the Müller cells. The distance between the two electrodes was 20 mm. A rectangular biphasic train of pulses (pulse duration, 1 ms; pulse frequency, 20 Hz; current intensity, 10 mA) was delivered between the electrodes continuously for 30 minutes through a stimulus isolation unit for delivery of a constant current (Stimulator SEN-7203; Nihon Kohden, Tokyo, Japan; Isolator A395R; World Precision Instruments, Sarasota, FL), as in our previous study.[13] The voltage between the electrodes was monitored on a 40-MHz oscilloscope (CS-4135A; Kenwood, Tokyo, Japan).

In control experiments, cells without ES were maintained on the bench for 30 minutes.

Microarray Analyses

To minimize the variations among the cell samples, the Müller cells from three dishes with or without ES were combined as the ES or control groups, respectively. Total RNA was isolated immediately after ES with an extraction reagent (RNeasy Mini Kit; Qiagen Japan, Tokyo, Japan) according to the manufacturer's protocols. The RNA samples were hybridized to a rat array containing 31,099 target probe sets (GeneChip Rat Genome 230 2.0 Array; Affymetrix Japan, Tokyo, Japan) and the following experiments were performed according to the manufacturer's recommendations.

The signal intensities were calculated with the microarray software (GeneChip Operating Software; Affymetrix Japan). If the raw signal intensities were <0.01, they were set to 0.01 according to the manufacturer's protocols. The raw intensity values in each chip were normalized to the 50th percentile of the measurements. Each gene was normalized to the median of that gene in the respective ES or control groups. Further analyses were performed with a second software program (GeneSpring 7.2 software; Agilent Technologies Japan, Tokyo, Japan) to compare the transcriptional inductions in the ES group with the control.

Quantitative Real-Time PCR

The mRNA levels of BDNF were determined by quantitative real-time PCR (RT-PCR) at 0, 1, 2, 3, and 6 hours after ES and calculated by the comparative C_T method.[23] β-Actin was used as the endogenous control. Total RNA was isolated by the method just described and was reverse transcribed to synthesize cDNA (First-Strand cDNA Synthesis System for Quantitative RT-PCR; Marligen Bioscience, Ijamsville, MD). RT-PCR was then performed (Prism 7900HT; Applied Biosystems [ABI] Japan, Tokyo, Japan) in a 384-well format by selecting primer and probe sets (*Taq*Man) from an online catalog (BDNF: *Taq*Man [ABI] Gene Expression Assay ID, Rn02531967_s1, Celera Annotation GenBank accession No. NM_178866.2; β-actin: ID Rn00667869_ml, No. NM_031144.2; http://www.ncbi.nlm.nih.gov/Genbank; provided in the public domain by the National Center for Biotechnology Information, Bethesda, MD). The sequences of the primers and probes are not disclosed. The thermal cycling conditions were: 50°C for 2 minutes, 95°C for 10 minutes, and 40 cycles at 95°C for 15 seconds and 60°C for 1 minute. Each measurement was performed in duplicate in six independent runs.

The expression of BDNF gene in the ES group was compared to that in the control group. The relative data are presented as the mean multiple of change (*x*-fold) ± SD calculated from the six separate experiments. The Wilcoxon signed rank test was used to analyze the statistical significance ($P < 0.05$) of differences between the median values.

Enzyme-Linked Immunosorbent Assay

Both extracellular and intracellular BDNF protein levels were measured at 3, 6, 12, 24, and 48 hours after ES by quantitative sandwich enzyme immunoassay (Chemicon International, Temecula CA) according to the manufacturer's instructions. This technique can measure both human and rat BDNF. The culture medium and the cell lysate were collected as the samples for extracellular and intracellular BDNF, respectively. To lyse the Müller cells, the cells were soaked in 200 μL of lysis buffer (RIPA buffer; Sigma-Aldrich) supplemented with a protease inhibitor cocktail (Protease Inhibitors Mixture for Protease and Esterase; Wako, Osaka, Japan). The lysate was centrifuged at 15,000 rpm for 10 minutes at 4°C, and the BDNF in the supernatant was measured as intracellular BDNF.

The optical density of each sample was measured at 450 nm with the correction wavelength set at 540 nm ($ARVO_{MX}$; PerkinElmer Japan, Kanagawa, Japan). Each measurement was performed in duplicate in six independent runs. The absolute protein amount of BDNF was calculated by the following equations:

$$\text{Extracellular BDNF (pg)} = \text{medium concentration (pg/mL)} \times 2 \text{ (mL, medium volume)},$$

$$\text{Intracellular BDNF (pg)} = \text{lysate concentration (pg/mL)} \times 0.2 \text{ (mL, lysate volume)},$$

and

$$\text{Total BDNF (pg)} = \text{sum of extra- and intracellular BDNF (pg)}.$$

The expression of the protein BDNF in the ES group was compared with that in the control group. The relative data are presented as the mean multiple of change ± SD calculated from six separate experiments. The Wilcoxon signed rank test was used to analyze the statistical significance ($P < 0.05$) of differences between the medians.

Quantitative Real-Time PCR with L-VDCC Blocker

The mRNA level of BDNF in Müller cells exposed to 1 μM nifedipine was determined by RT-PCR at 3 hours after ES and compared with that in Müller cells without nifedipine. Briefly, 1 μM nifedipine was added to the culture medium immediately before the start of ES. The dose of nifedipine was enough to block the Ca^{2+} influx via L-VDCCs.[13] ES was applied to Müller cells, and thereafter the medium of the dishes with and without ES was replaced by 2 mL fresh culture medium.

The mRNA level of BDNF in Müller cells without ES and nifedipine was normalized to 1, and the relative data are presented as the mean multiple of change ± SD calculated from twelve separate experiments. The Kruskal-Wallis one-way ANOVA on ranks was used to analyze the statistical significance ($P < 0.05$) of the differences among the median values, followed by Dunn's method to determine significant differences between each group.

Results

These experiments were conducted on passage 1 Müller cells because the primary-culture cells were contaminated by many other cell types, and preliminary assays by RT-PCR showed marked variations in the expression levels of several genes among the culture dishes (data not shown). Examination of the cells with an optical microscope showed that the morphologic appearance of the Müller cells did not change after the different experimental procedures.

Microarray Analyses

In our earlier study,[13] a Ca^{2+} influx into Müller cells was detected immediately after the beginning of ES, and the mRNA of IGF-1 was upregulated at the cessation of ES. Thus, to evaluate the direct effect of ES on the changes in gene expression, we performed microarray analyses on cells isolated immediately after ES.

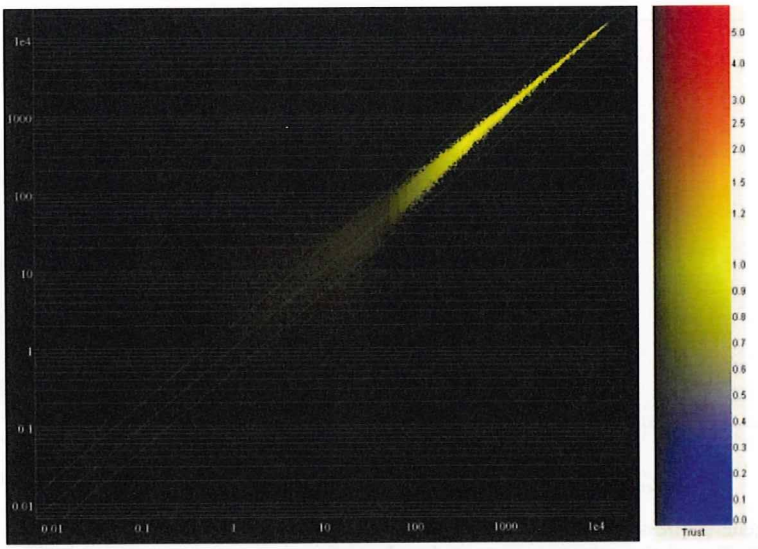

A

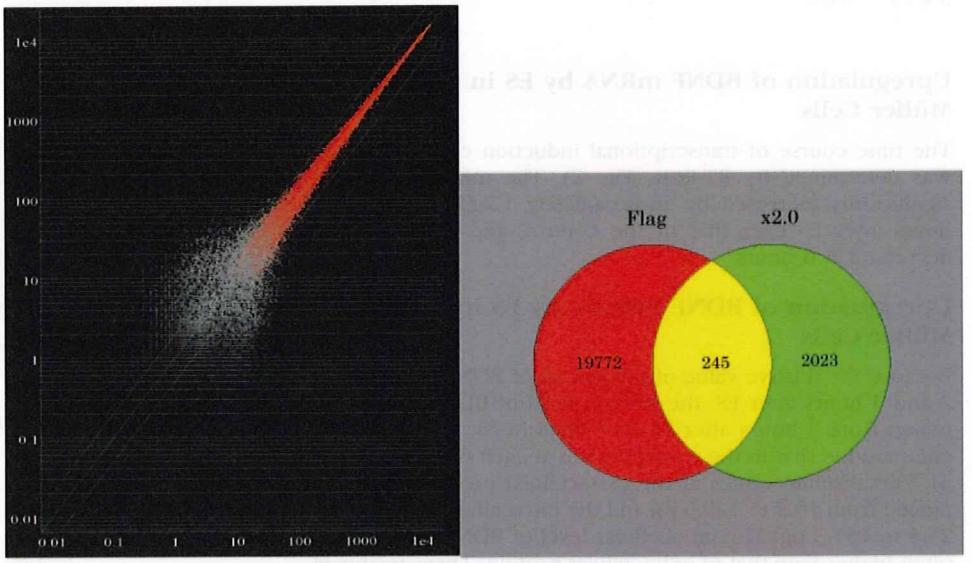

B

FIGURE 1. Results of microarray analyses. The horizontal and vertical axes represent the signal intensity of the genes expressed in the control and ES groups, respectively. (**A**) Signal intensity image plot of all gene expressions (31,099 probes). For each probe, the ratio of the signal intensity in the ES group to that in control is represented by a color, according to the vertical strip. (**B**) The circle of Flag contains the genes with signals that were "present" or "marginal" in the ES or control groups or both. The circle of ×2.0 holds the genes showing a more than twofold signal intensity in ES compared with the control. *Left*: signal intensity image of the probes, which corresponds to the pie chart.

The results showed that 7.3% (2268) of the probes expressed more than a twofold higher signal intensity in the ES group than in the control (Fig. 1A). The probes whose signals were absent in both the ES and control groups were not analyzed, according to the manufacturer's recommendations. The number of probes showing sufficient intensities that were more than two times higher in the ES than in the control was 245 (Fig. 1B). The genes associated with nervous system development were selected and are listed in Table 1. The most well-known neurotrophic factor was BDNF, with a gene expression that changed from absent in the control to a 2.6-fold increase in the ES group. Thus, the following experiments were focused on BDNF.

TABLE 1. Results of Microarray Analyses Immediately after ES

Description	GenBank Accession No.	Normalized Signal Intensity in Control	Flags of Control	Normalized Signal Intensity in ES	Flags of ES
Dihydropyrimidinase-like 3	AI059953	1.00	A	2.02	P
Zinc finger and BTB domain containing 16	BG371725	1.00	A	2.15	P
Ectodermal-neural cortex 1	AA997271	1.00	M	2.19	A
Brain derived neurotrophic factor	X67108	1.00	A	2.58	P
Stathmin-like 3	NM_024346	1.00	A	3.31	M
UDP galactosyltransferase 8	L21698	1.00	A	13.77	P

A, absent; M, marginal; P, present.

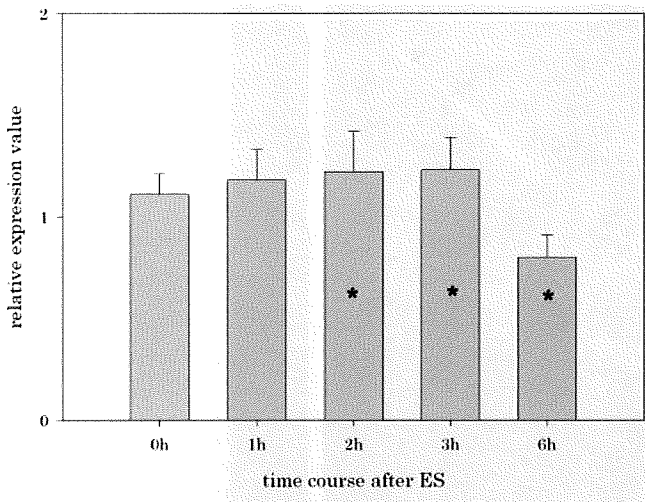

FIGURE 2. Relative gene expressions of BDNF after ES at 10 mA determined by RT-PCR. The relative values are presented as the mean multiple of change (*x*-fold) ± SD calculated from six separate experiments. Statistical analysis was performed by the Wilcoxon signed rank test (*$P < 0.05$).

Upregulation of BDNF mRNA by ES in Cultured Müller Cells

The time course of transcriptional induction of BDNF by ES was determined by RT-PCR (Fig. 2). The mRNA level was significantly increased by approximately 1.2-fold at 2 and 3 hours after ES over that of the control, and the level was decreased at 6 hours.

Upregulation of BDNF Protein by ES in Cultured Müller Cells

Because the relative value of the mRNA of BDNF increased at 2 and 3 hours after ES, the protein level of BDNF was determined from 3 hours after ES. The level in the ES group was compared to that in the control group at each time point (Fig. 3). The absolute values of the extracellular proteins of BDNF ranged from 10.2 to 129.6 pg and the intracellular values from 25.5 to 151.3 pg. The intracellular level of BDNF protein was often higher than that of extracellular protein. These relatively large variations were probably due to the different number of cultured Müller cells between the experimental runs.

The intracellular protein level of BDNF in the experimental cells was significantly increased (>1.4-fold) at 6 hours after ES compared with that in the control cells, whereas the extracellular level did not change significantly at any time point. The total protein was significantly upregulated (by ~1.3-fold) at 6 hours after ES.

Suppression of BDNF mRNA by Blocking L-VDCCs in Cultured Müller Cells

In earlier work, we showed that ES induced the transcription of IGF-1 by Ca^{2+} influx via L-VDCCs in cultured Müller cells.[13] Because Ca^{2+} ions are one of the common second messengers,[14] we hypothesized that the transcriptional induction of BDNF also depends largely on the Ca^{2+} influx through L-VDCCs. A common pharmacologic hallmark of L-VDCCs is their sensitivity to dihydropyridines.[24] Thus, the gene expression of BDNF was determined at 3 hours after ES by RT-PCR in Müller cells loaded with 1 μM nifedipine, a dihydropyridine calcium channel blocker (Fig. 4).

The mRNA level of BDNF was approximately 0.5-fold at 0 mA with nifedipine and 0.4-fold at 10 mA with nifedipine compared with that of 0 mA (control). Statistical significance

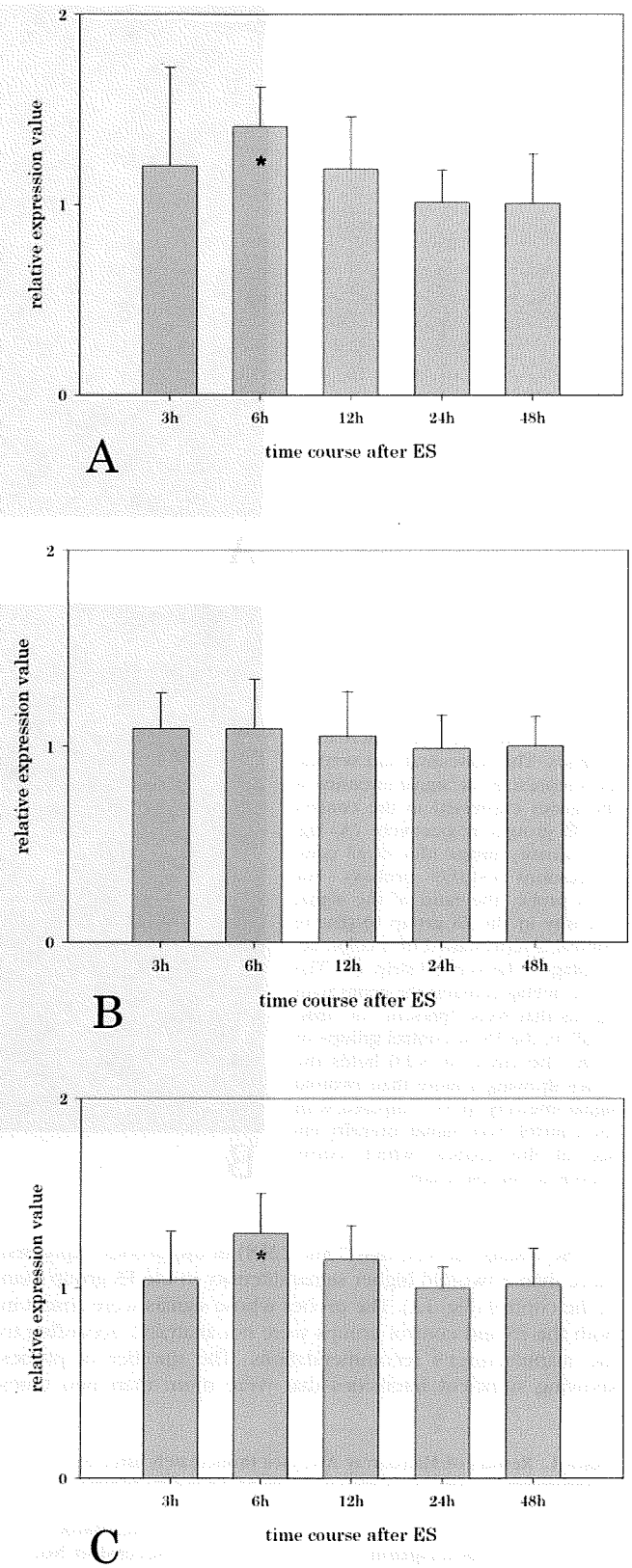

FIGURE 3. Relative protein expressions of BDNF after ES at 10 mA determined by ELISA. The relative values are presented as the mean multiple of change (*x*-fold) ± SD calculated from six separate experiments. Statistical analysis was performed by Wilcoxon signed rank test (*$P < 0.05$). (**A**) Intracellular protein level of BDNF. The absolute levels of intracellular BDNF ranged from 25.5 to 151.3 pg. (**B**) Extracellular level of BDNF. The absolute extracellular level of BDNF ranged from 10.2 to 129.6 pg. (**C**) Total level of BDNF. The absolute level of total BDNF ranged from 60.0 to 249.3 pg.

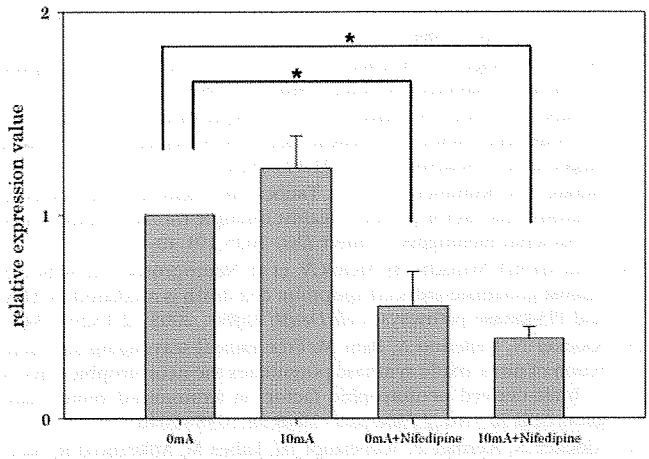

FIGURE 4. Relative gene expressions of BDNF with or without 1 μM nifedipine at 3 hours after 10 mA ES, determined by RT-PCR. The relative data are presented as the mean multiples of change (x-fold) ± SD in 12 separate experiments. Statistical analysis was performed by Kruskal-Wallis one-way ANOVA on ranks, followed by the Dunn test (*$P < 0.05$).

was detected among these four groups ($P = < 0.001$; Kruskal-Wallis one-way ANOVA on ranks), and the levels after exposure to nifedipine were significantly lower than that with 0 mA ($P < 0.05$; Dunn's method). These results indicated that the transcription of BDNF in cultured Müller cells was upregulated by ES, was most likely due to Ca^{2+} influx into the cells via L-VDCCs, and was downregulated by the application of nifedipine, which prevented Ca^{2+} influx via L-VDCCs.

DISCUSSION

To investigate the direct effect of ES on the production of neurotrophic factors from Müller cells, ES was applied to cultured Müller cells. The major findings were that both the message and protein levels of BDNF in cultured Müller cells were upregulated by ES, and that the transcriptional induction of BDNF is fully depressed by the application of an L-VDCC blocker. These findings suggest that the transcriptional induction by ES depends largely on Ca^{2+} influx through L-VDCCs.

Although BDNF was first purified from brain cells,[25] it has been shown to play crucial roles, not only in CNS[26–28] but also in the retina. Recent studies have demonstrated that BDNF promoted the survival of RGCs in different models.[29–33] Furthermore, Paskowitz et al.[34] demonstrated that BDNF increased photoreceptor survival after verteporfin photodynamic therapy, indicating that BDNF had a neuroprotective effect on the photoreceptors. These findings support the conclusion that BDNF acts as a neurotrophic agent in the retina.

However, one crucial question regarding the clinical application of BDNF is how to deliver it to the retinal neurons. Previous studies[29–34] have demonstrated that exogenous BDNF, delivered by intravitreous injections, had a protective effect on retinal neurons. However, exogenous BDNF had a transient and limited protective effect, and repeated applications were necessary, which can have adverse effects on the retina. On this point, we have already developed a system of transcorneal ES to the retina and showed the protective effect on the eyes with optic nerve diseases without serious complications.[35] These results indicate the possibility that ES may safely induce the production of endogenous BDNF from Müller cells to promote the survival of retinal neurons.

In this study, the extracellular protein level of BDNF did not increase at any time point. The reason for this is still not clear, but one possibility is that BDNF behaves as an autocrine factor in cultures of pure Müller cells. An earlier study demonstrated that Müller cells not only synthesize BDNF but also express TrkB, the specific receptor of BDNF.[36] These results indicate that BDNF secreted from Müller cells may be expanded by an autocrine mechanism and that the transcriptional induction of BDNF may be suppressed at 6 hours by negative feedback of the increased protein of BDNF.

The mechanism of how ES stimulates L-VDCCs in cultured Müller cells is not fully understood. It is well known that Ca^{2+}-regulated gene expression plays a critical role in diverse neural functions and that the activation of L-VDCCs is required for depolarization-mediated gene induction.[20] Most studies that have examined mechanisms of activity-dependent gene expression have used chronic membrane depolarization to raise intracellular calcium levels and stimulate gene expression.[21] Further studies are needed to determine the mechanisms involved in the gene expression of BDNF by ES in Müller cells.

One of the limitations of this study is that the microarray analyses were performed at only one time point, immediately after ES. In fact, the mRNA level of BDNF determined by RT-PCR was higher at 2 and 3 hours than at 0 hours after ES, although the transcriptional induction depended mainly on Ca^{2+} influx through L-VDCCs, similar to that for IGF-1. Thus, we cannot exclude the possibility that other neurotrophic factors may have been induced by the ES.

In summary, we have demonstrated the direct effect of ES on BDNF production in cultured rat Müller cells. Our findings raise the possibility that ES may deliver endogenous BDNF from Müller cells without serious complications and promote the survival of retinal neurons.

Acknowledgments

The authors thank Takayuki Harada for crucial comments on this study.

References

1. Otori Y, Shimada S, Tanaka K, Ishimoto I, Tano Y, Tohyama M. Marked increase in glutamate-aspartate transporter (GLAST/GluT-1) mRNA following transient retinal ischemia. *Brain Res Mol Brain Res.* 1994;27:310–314.
2. Derouiche A, Rauen T. Coincidence of L-glutamate/L-aspartate transporter (GLAST) and glutamine synthetase (GS) immunoreactions in retinal glia: evidence for coupling of GLAST and GS in transmitter clearance. *J Neurosci Res.* 1995;42:131–143.
3. Kitano S, Morgan J, Caprioli J. Hypoxic and excitotoxic damage to cultured rat retinal ganglion cells. *Exp Eye Res.* 1996;63:105–112.
4. Lehre KP, Davanger S, Danbolt NC. Localization of the glutamate transporter protein GLAST in rat retina. *Brain Res.* 1997;744:129–137.
5. Matsui K, Hosoi N, Tachibana M. Active role of glutamate uptake in the synaptic transmission from retinal nonspiking neurons. *J Neurosci.* 1999;19:6755–6766.
6. Riepe RE, Norenburg MD. Müller cell localization of glutamine synthetase in rat retina. *Nature.* 1977;268:654–655.
7. Curtis DR, Watkins JC. The excitation and depression of spinal neurones by structurally related amino acids. *J Neurochem.* 1960;6:117–141.
8. Seki M, Tanaka T, Sakai Y, et al. Müller cells as a source of brain-derived neurotrophic factor in the retina: noradrenaline upregulates brain-derived neurotrophic factor levels in cultured rat Müller cells. *Neurochem Res.* 2005;30:1163–1170.
9. Wilson RB, Kunchithapautham K, Rohrer B. Paradoxical role of BDNF: $BDNF^{+/-}$ retinas are protected against light damage-mediated stress. *Invest Ophthalmol Vis Sci.* 2007;48:2877–2886.
10. Cao W, Wen R, Li F, Cheng T, Steinberg RH. Induction of basic fibroblast growth factor mRNA by basic fibroblast growth factor in Müller cells. *Invest Ophthalmol Vis Sci.* 1997;38:1358–1366.
11. Harada T, Harada C, Nakayama N, et al. Modification of glial-neuronal cell interactions prevents photoreceptor apoptosis during light-induced retinal degeneration. *Neuron.* 2000;26:533–541.